

Klimaänderung II

0. Rückblick auf das vergangene Wintersemester

Robert Sausen

Institut für Physik der Atmosphäre
Deutsches Zentrum für Luft- und Raumfahrt
Oberpfaffenhofen

Vorlesung SS 2023

LMU München



Knowledge for Tomorrow

Technical information

- <http://www.pa.op.dlr.de/~RobertSausen/vorlesung/index.html>
 - Most recent update on the lecture
 - Slides of the lecture (with some delay)

 - See also LSF <https://lsf.verwaltung.uni-muenchen.de/>

- Contact: robert.sausen@dlr.de

- Further information:
 - www.ipcc.ch
 - www.de-ipcc.de



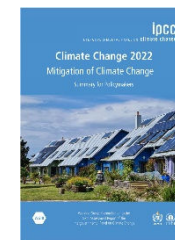
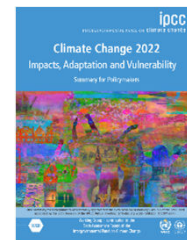
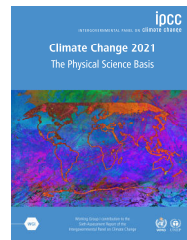
Questions

- Has there been a climate change ?
- What is the impact of man ?
- How will the climate develop in the future ?
- What is necessary to limit climate change?



An important source of knowledge: IPCC Assessment Reports

Central results of the recent IPCC Assessment Report (Sixth Assessment Report "AR6", 2021)



Central results of the recent Fifth IPCC Assessment Report ("AR5", 2013/2014)



Results from the IPCC Special Report (SR15) "Global Warming of 1.5 °C"

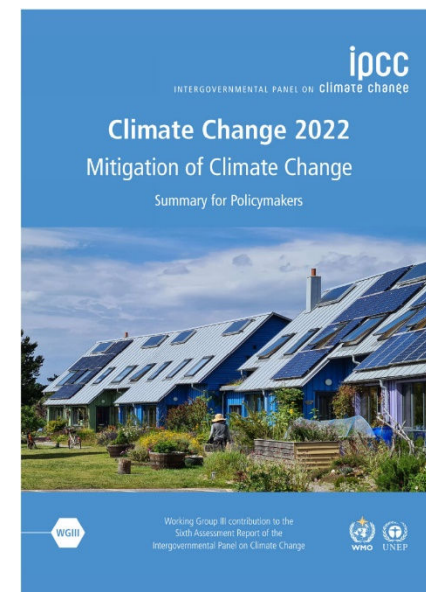
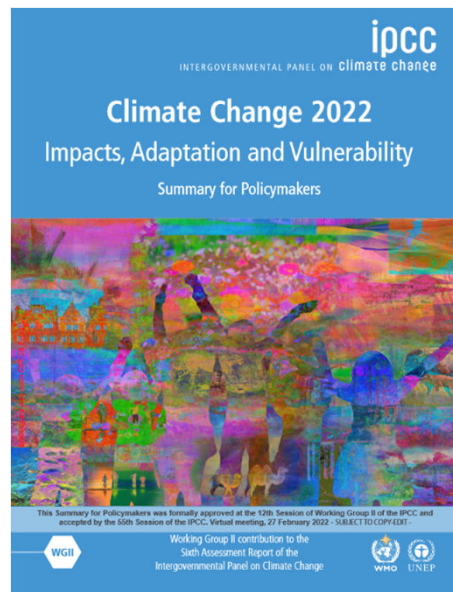
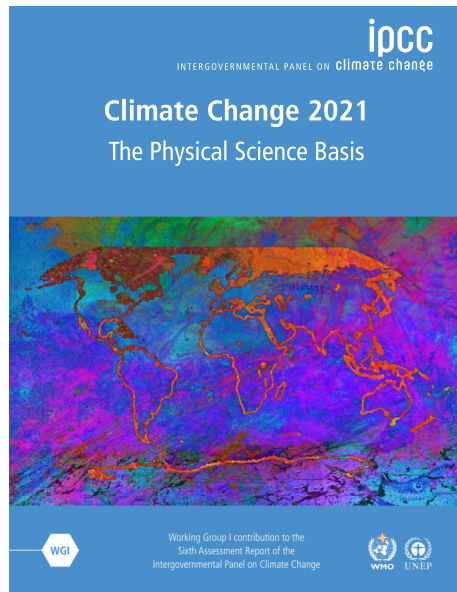


www.ipcc.ch
www.de-ipcc.de



An important source of knowledge: IPCC Assessment Reports

Central results of the recent IPCC Assessment Report (Sixth Assessment Report "AR6", 2021)



Sir John Houghton

(30 December 1931 – 15 April 2020)

Dedication

Sir John Houghton
(30 December 1931 – 15 April 2020)



The Working Group I Contribution to the Sixth Assessment Report of the Intergovernmental Panel on Climate Change (IPCC) *Climate Change 2021: The Physical Science Basis* is dedicated to the memory of Sir John Houghton, who was one of the key figures in the creation of the IPCC in 1988, and served as Chair and Co-Chair of Working Group I for the IPCC's first three assessment reports from 1988 to 2002.

Sir John's work was a major factor in the award of the Nobel Peace Prize to the IPCC in 2007, shared with former U.S. Vice-President Al Gore. He contributed to the development of climate science and building international cooperation based upon climate research. Sir John played a key role in ensuring a robust science-policy interface, used in the IPCC process, but his role in international scientific research extended beyond the IPCC, for instance in contributing to the establishment of the World Climate Research Programme, which he chaired from 1982 to 1984.

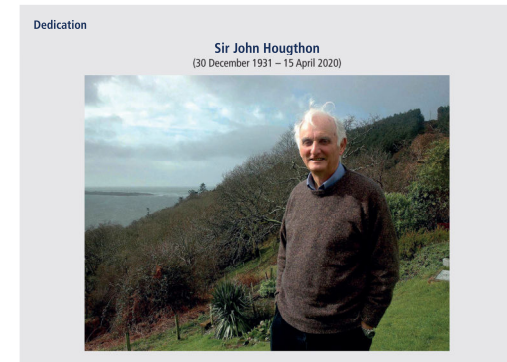
Sir John was a brilliant communicator among scientific colleagues, policymakers and the public at large, explaining the fact and threat of climate change with clarity and directness.

IPCC 2021



Sir John Houghton

(30 December 1931 – 15 April 2020)



The Working Group I Contribution to the Sixth Assessment Report of the Intergovernmental Panel on Climate Change (IPCC) *Climate Change 2021: The Physical Science Basis* is dedicated to the memory of Sir John Houghton, who was one of the key figures in the creation of the IPCC in 1988, and served as Chair and Co-Chair of Working Group I for the IPCC's first three assessment reports from 1988 to 2002.

Sir John's work was a major factor in the award of the Nobel Peace Prize to the IPCC in 2007, shared with former U.S. Vice-President Al Gore. He contributed to the development of climate science and building international cooperation based upon climate research. Sir John played a key role in ensuring a robust science-policy interface, used in the IPCC process, but his role in international scientific research extended beyond the IPCC, for instance in contributing to the establishment of the World Climate Research Programme, which he chaired from 1982 to 1984.

Sir John was a brilliant communicator among scientific colleagues, policymakers and the public at large, explaining the fact and threat of climate change with clarity and directness.



What is IPCC (Intergovernmental Panel on Climate Change) 1

The IPCC provides regular assessments of the scientific basis of climate change, its impacts and future risks, and options for adaptation and mitigation.

Created in 1988 by the World Meteorological Organization (WMO) and the United Nations Environment Programme (UNEP), the objective of the IPCC is to provide governments at all levels with scientific information that they can use to develop climate policies. IPCC reports are also a key input into international climate change negotiations. The IPCC is an organization of governments that are members of the United Nations or WMO. The IPCC currently has 195 members. Thousands of people from all over the world contribute to the work of the IPCC. For the assessment reports, IPCC scientists volunteer their time to assess the thousands of scientific papers published each year to provide a comprehensive summary of what is known about the drivers of climate change, its impacts and future risks, and how adaptation and mitigation can reduce those risks. An open and transparent review by experts and governments around the world is an essential part of the IPCC process, to ensure an objective and complete assessment and to reflect a diverse range of views and expertise. Through its assessments, the IPCC identifies the strength of scientific agreement in different areas and indicates where further research is needed. The IPCC does not conduct its own research.

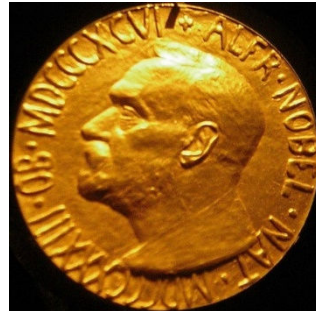
What is IPCC (Intergovernmental Panel on Climate Change) 2

"IPCC assessments provide a scientific basis for governments at all levels to develop climate related policies, and they underlie negotiations at the UN Climate Conference – the United Nations Framework Convention on Climate Change (UNFCCC). **The assessments are policy-relevant but not policy-prescriptive:** they may present projections of future climate change based on different scenarios and the risks that climate change poses and discuss the implications of response options, **but they do not tell policymakers what actions to take.**"

IPCC, 2013



IPCC was awarded the Nobel Peace Prize in 2007

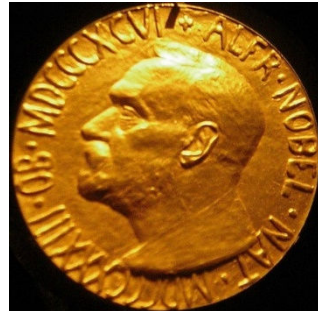


The Nobel Peace Prize 2007 was awarded to the Intergovernmental Panel on Climate Change (IPCC) and Albert Arnold (Al) Gore Jr.

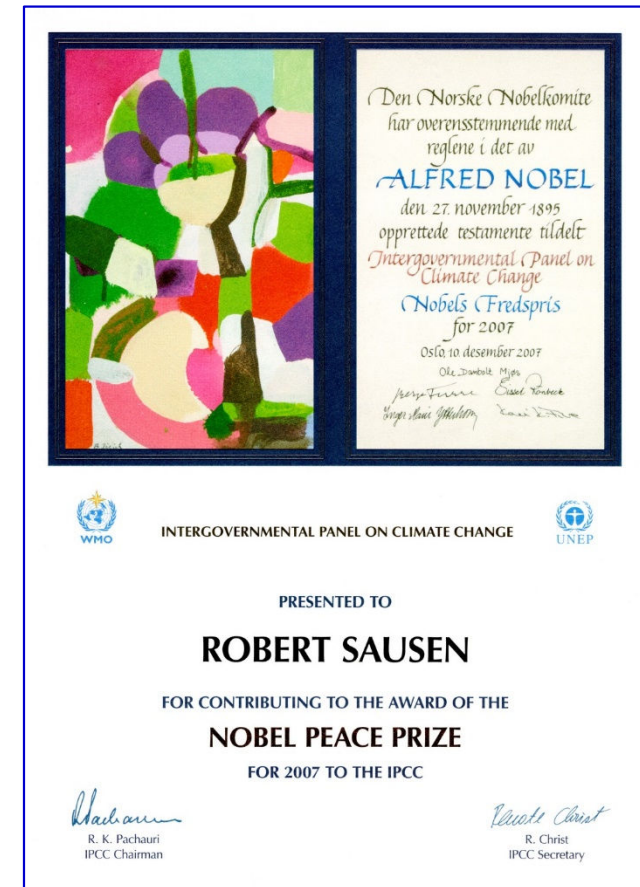
"for their efforts to build up and disseminate greater knowledge about man-made climate change, and to lay the foundations for the measures that are needed to counteract such change"



IPCC was awarded the Nobel Peace Prize in 2007



The Nobel Peace Prize 2007 was awarded to the Intergovernmental Panel on Climate Change (IPCC) and Albert Arnold (Al) Gore Jr. "for their efforts to build up and disseminate greater knowledge about man-made climate change, and to lay the foundations for the measures that are needed to counteract such change"



The Nobel Prize in Physics 2021 has been awarded to Syukuro Manabe, Klaus Hasselmann and Giorgio Parisi

Syukuro Manabe Facts



Ill. Niklas Elmehed © Nobel Prize Outreach

Syukuro Manabe
The Nobel Prize in Physics 2021

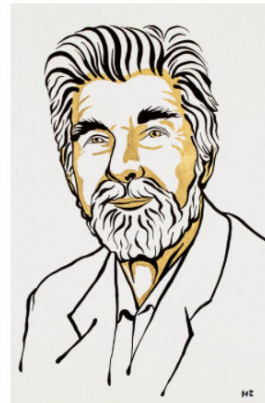
Born: 21 September 1931, Shingu, Ehime Prefecture, Japan

Affiliation at the time of the award: Princeton University, Princeton, NJ, USA

Prize motivation: "for the physical modelling of Earth's climate, quantifying variability and reliably predicting global warming."

Prize share: 1/4

Klaus Hasselmann Facts



Ill. Niklas Elmehed © Nobel Prize Outreach

Klaus Hasselmann
The Nobel Prize in Physics 2021

Born: 25 October 1931, Hamburg, Germany

Affiliation at the time of the award: Max Planck Institute for Meteorology, Hamburg, Germany

Prize motivation: "for the physical modelling of Earth's climate, quantifying variability and reliably predicting global warming."

Prize share: 1/4



Contents of IPCC AR 6 2021

Working Group I: the Physical Science Basis

Contents	
Front Matter	Foreword v
	Preface vii
	Dedication xiii
SPM	Summary for Policymakers 3
TS	Technical Summary 35
Chapters	Chapter 1 Framing, Context, and Methods 147
	Chapter 2 Changing State of the Climate System 287
	Chapter 3 Human Influence on the Climate System 423
	Chapter 4 Future Global Climate: Scenario-based Projections and Near-term Information 553
	Chapter 5 Global Carbon and Other Biogeochemical Cycles and Feedbacks 673
	Chapter 6 Short-lived Climate Forcers 817
	Chapter 7 The Earth's Energy Budget, Climate Feedbacks and Climate Sensitivity 923
	Chapter 8 Water Cycle Changes 1055
	Chapter 9 Ocean, Cryosphere and Sea Level Change 1211
	Chapter 10 Linking Global to Regional Climate Change 1363
	Chapter 11 Weather and Climate Extreme Events in a Changing Climate 1513
	Chapter 12 Climate Change Information for Regional Impact and for Risk Assessment 1767
	Atlas 1927
Annexes	Annex I Observational Products 2061
	Annex II Models 2087
	Annex III Tables of Historical and Projected Well-mixed Greenhouse Gas Mixing Ratios and Effective Radiative Forcing of All Climate Forcers 2139
	Annex IV Modes of Variability 2153
	Annex V Monsoons 2193
	Annex VI Climatic Impact-driver and Extreme Indices 2205
	Annex VII Glossary 2215
	Annex VIII Acronyms 2257
	Annex IX Contributors to the IPCC WGI Sixth Assessment Report 2267
	Annex X Expert Reviewers of the IPCC Sixth Assessment Report 2287
	Index 2339

IPCC 2021



Front Matter

Foreword

Preface

Dedication

SPM

Summary for Policymakers

TS

Technical Summary

Chapters

Chapter 1 Framing, Context, and Methods

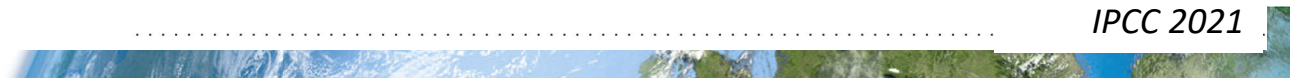
Chapter 2 Changing State of the Climate System

IPCC 2021



Chapters

Chapter 1	Framing, Context, and Methods
Chapter 2	Changing State of the Climate System
Chapter 3	Human Influence on the Climate System
Chapter 4	Future Global Climate: Scenario-based Projections and Near-term Information
Chapter 5	Global Carbon and Other Biogeochemical Cycles and Feedbacks
Chapter 6	Short-lived Climate Forcers
Chapter 7	The Earth's Energy Budget, Climate Feedbacks and Climate Sensitivity
Chapter 8	Water Cycle Changes
Chapter 9	Ocean, Cryosphere and Sea Level Change
Chapter 10	Linking Global to Regional Climate Change
Chapter 11	Weather and Climate Extreme Events in a Changing Climate
Chapter 12	Climate Change Information for Regional Impact and for Risk Assessment
Atlas <i>IPCC 2021</i>



Annexes

Atlas

Annex I Observational Products

Annex II Models

Annex III Tables of Historical and Projected Well-mixed Greenhouse Gas Mixing Ratios and Effective Radiative Forcing of All Climate Forcers

Annex IV Modes of Variability

Annex V Monsoons

Annex VI Climatic Impact-driver and Extreme Indices

Annex VII Glossary

Annex VIII Acronyms

Annex IX Contributors to the IPCC WGI Sixth Assessment Report

Annex X Expert Reviewers of the IPCC Sixth Assessment Report

Index



Klimaänderung I

1. Rahmen, Kontext, Methoden

Robert Sausen

Institut für Physik der Atmosphäre
Deutsches Zentrum für Luft- und Raumfahrt
Oberpfaffenhofen

Vorlesung WS 2022/23

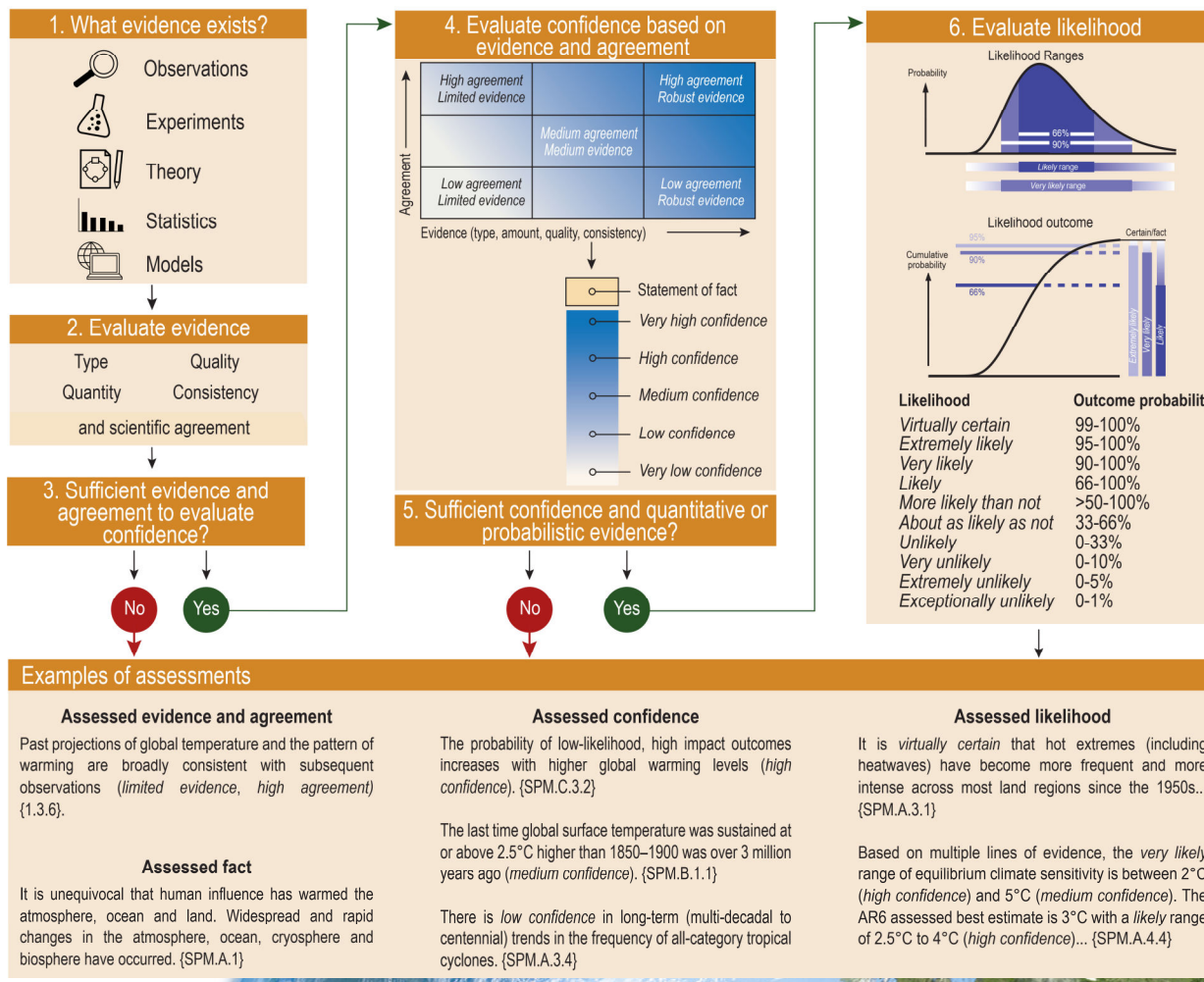
LMU München

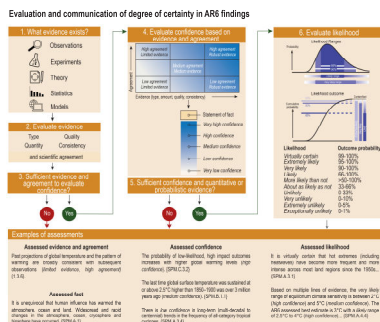


Knowledge for Tomorrow



Evaluation and communication of degree of certainty in AR6 findings





4. Evaluate confidence based on evidence and agreement

Agreement ↑	High agreement Limited evidence		High agreement Robust evidence
		Medium agreement Medium evidence	
	Low agreement Limited evidence		Low agreement Robust evidence

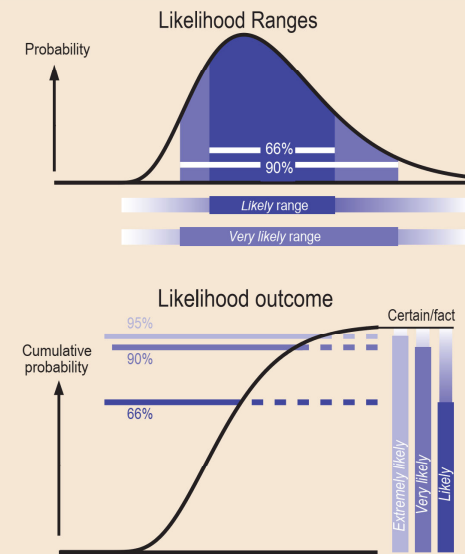
Evidence (type, amount, quality, consistency) →

- Statement of fact
- Very high confidence
- High confidence
- Medium confidence
- Low confidence
- Very low confidence

5. Sufficient confidence and quantitative or probabilistic evidence?



6. Evaluate likelihood



Likelihood	Outcome probability
Virtually certain	99-100%
Extremely likely	95-100%
Very likely	90-100%
Likely	66-100%
More likely than not	>50-100%
About as likely as not	33-66%
Unlikely	0-33%
Very unlikely	0-10%
Extremely unlikely	0-5%
Exceptionally unlikely	0-1%

Climate science milestones between 1817-2021

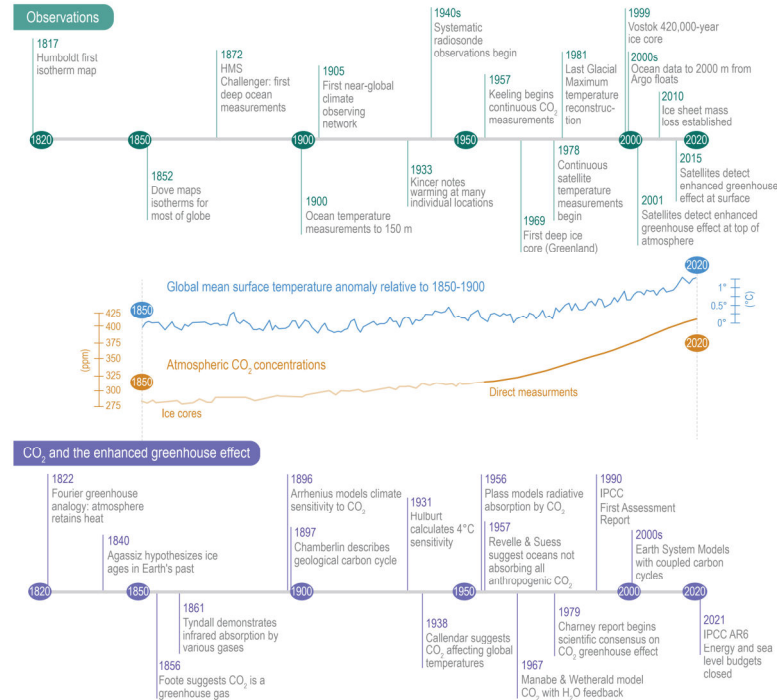
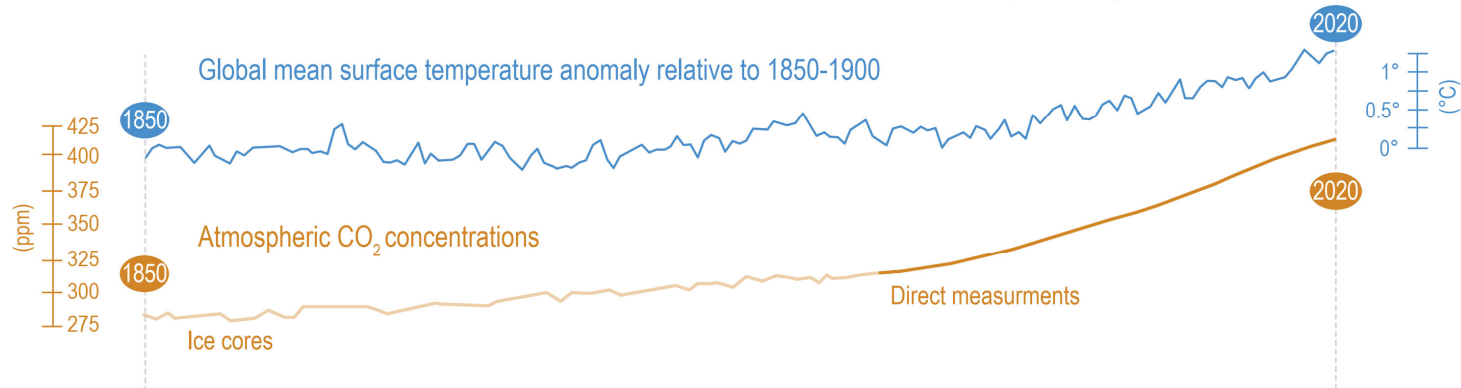
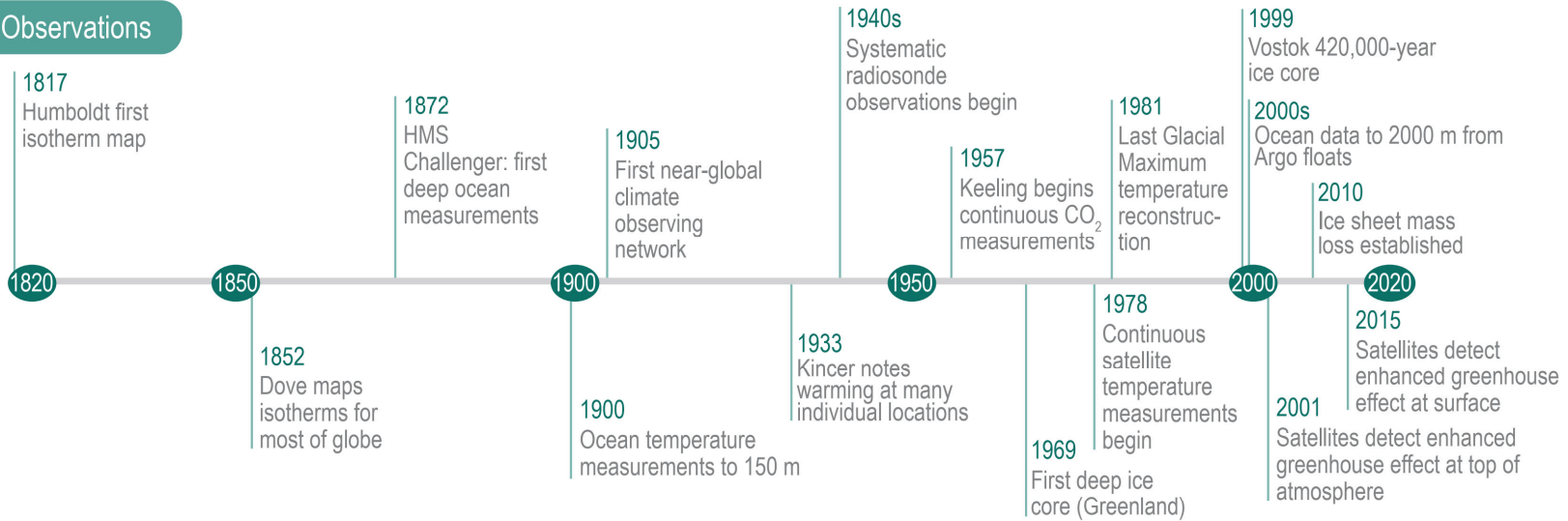
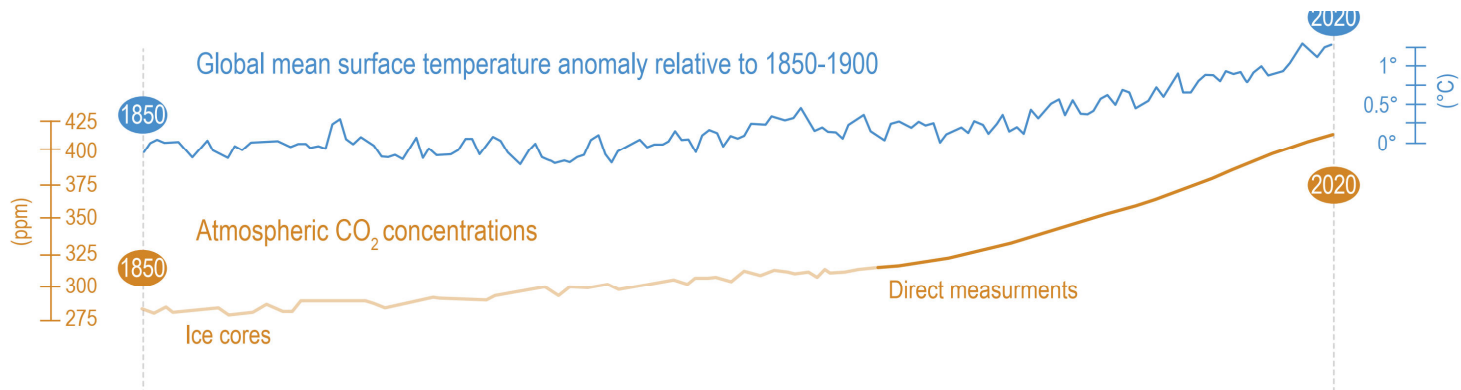


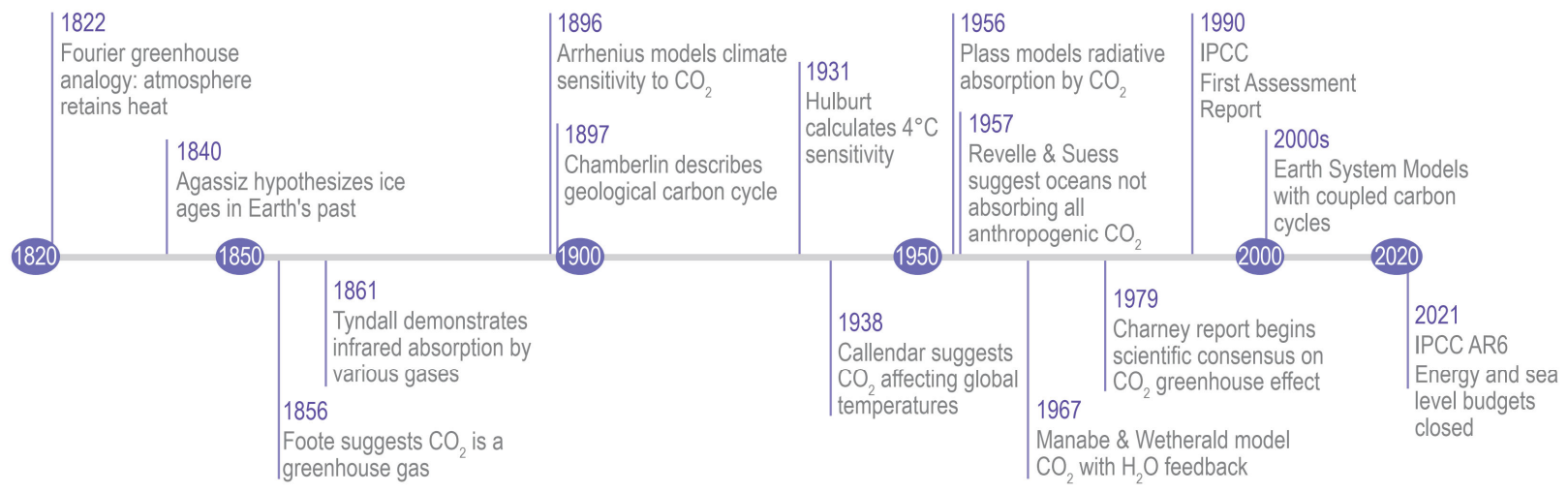
Figure 1.6 | Climate science milestones, between 1817 and 2021. Top: Milestones in observations. **Middle:** Curves of global surface air temperature (GMST) anomaly relative to 1850–1900, using HadCRUT5 (Morice et al., 2021); atmospheric CO₂ concentrations from Antarctic ice cores (Lüthi et al., 2008; Bereiter et al., 2015); direct air measurements from 1957 onwards (see Figure 1.4 for details; Tans and Keeling, 2020). **Bottom:** Milestones in scientific understanding of the CO₂-enhanced greenhouse effect. Further details on each milestone are available in Section 1.3, and in Chapter 1 of AR4 (Le Treut et al., 2007).

Observations

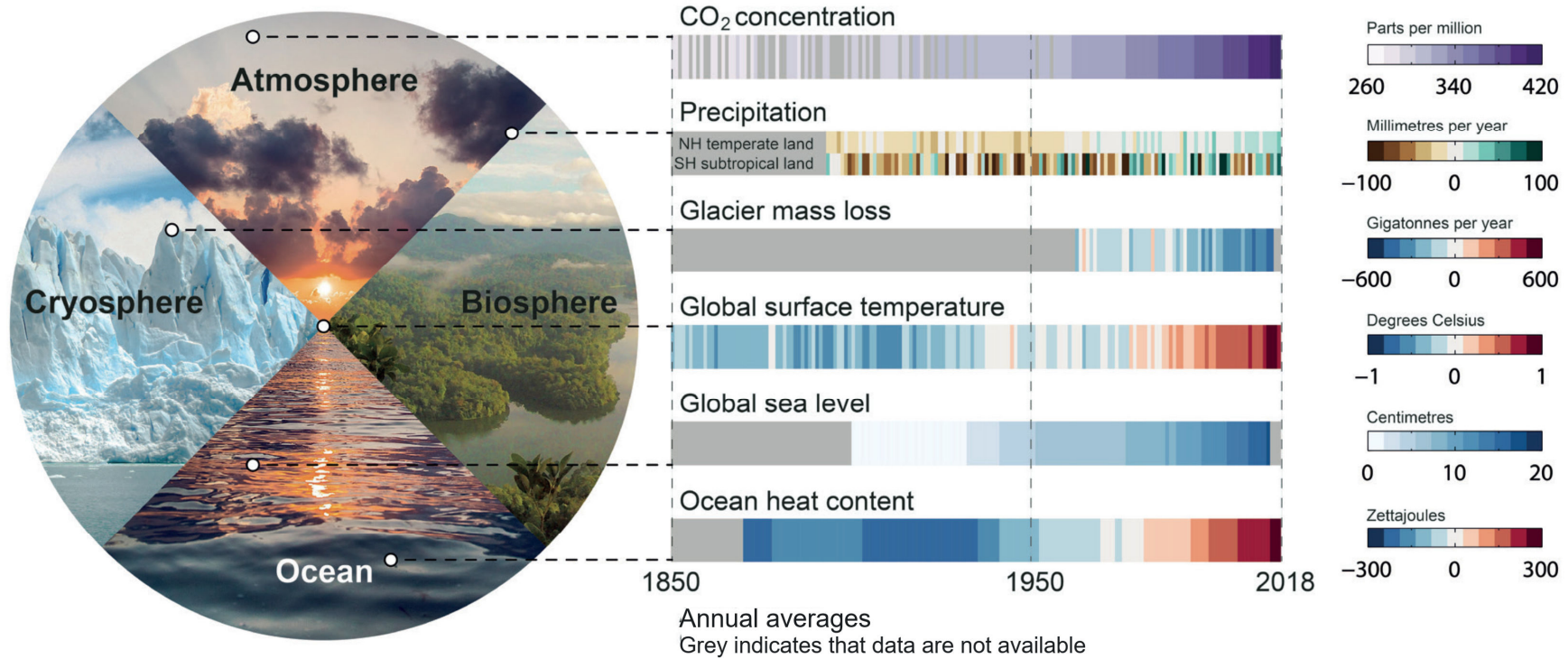




CO₂ and the enhanced greenhouse effect



Changes are occurring throughout the climate system



IPCC 2021, Chap. 1

Figure 1.4 | Changes are occurring throughout the climate system. **Left:** Main realms of the climate system: atmosphere, biosphere, cryosphere and ocean. **Right:** Six key indicators of ongoing changes since 1850, or the start of the observational or assessed record, through 2018. Each stripe indicates the global (except for precipitation which shows two latitude band means), annual mean anomaly for a single year, relative to a multi-year baseline (except for CO₂ concentration and glacier mass loss, which are absolute values). Grey indicates that data are not available. Datasets and baselines used are: (i) CO₂: Antarctic ice cores (Lüthi et al., 2008; Bereiter et al., 2015) and direct air measurements (Tans and Keeling, 2020) (see Figure 1.5 for details); (ii) precipitation: Global Precipitation Climatology Centre (GPCC) V8 (updated from Becker et al., 2013), baseline 1961–1990 using land areas only with latitude bands 33°N–66°N and 15°S–30°S; (iii) glacier mass loss: Zemp et al. (2019); (iv) global surface air temperature (GMST): HadCRUT5 (Morice et al., 2021), baseline 1961–1990; (v) sea level change: (Dangendorf et al., 2019), baseline 1900–1929; (vi) ocean heat content (model–observation hybrid): Zanna et al. (2019), baseline 1961–1990. Further details on data sources and processing are available in the chapter data table (Table 1.SM.1).

Klimaänderung I

2. Das sich verändernde Klimasystem

Robert Sausen

Institut für Physik der Atmosphäre
Deutsches Zentrum für Luft- und Raumfahrt
Oberpfaffenhofen

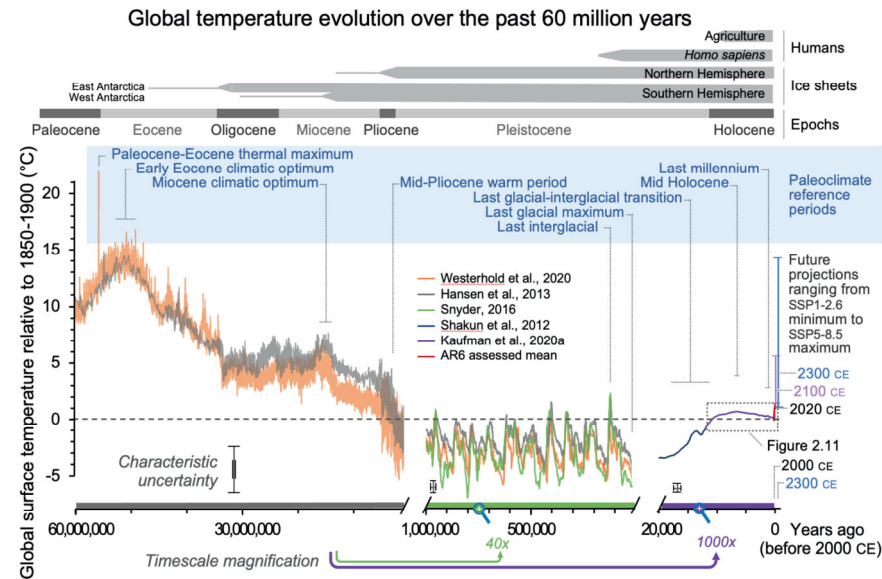
Vorlesung WS 2022/23

LMU München



Knowledge for Tomorrow

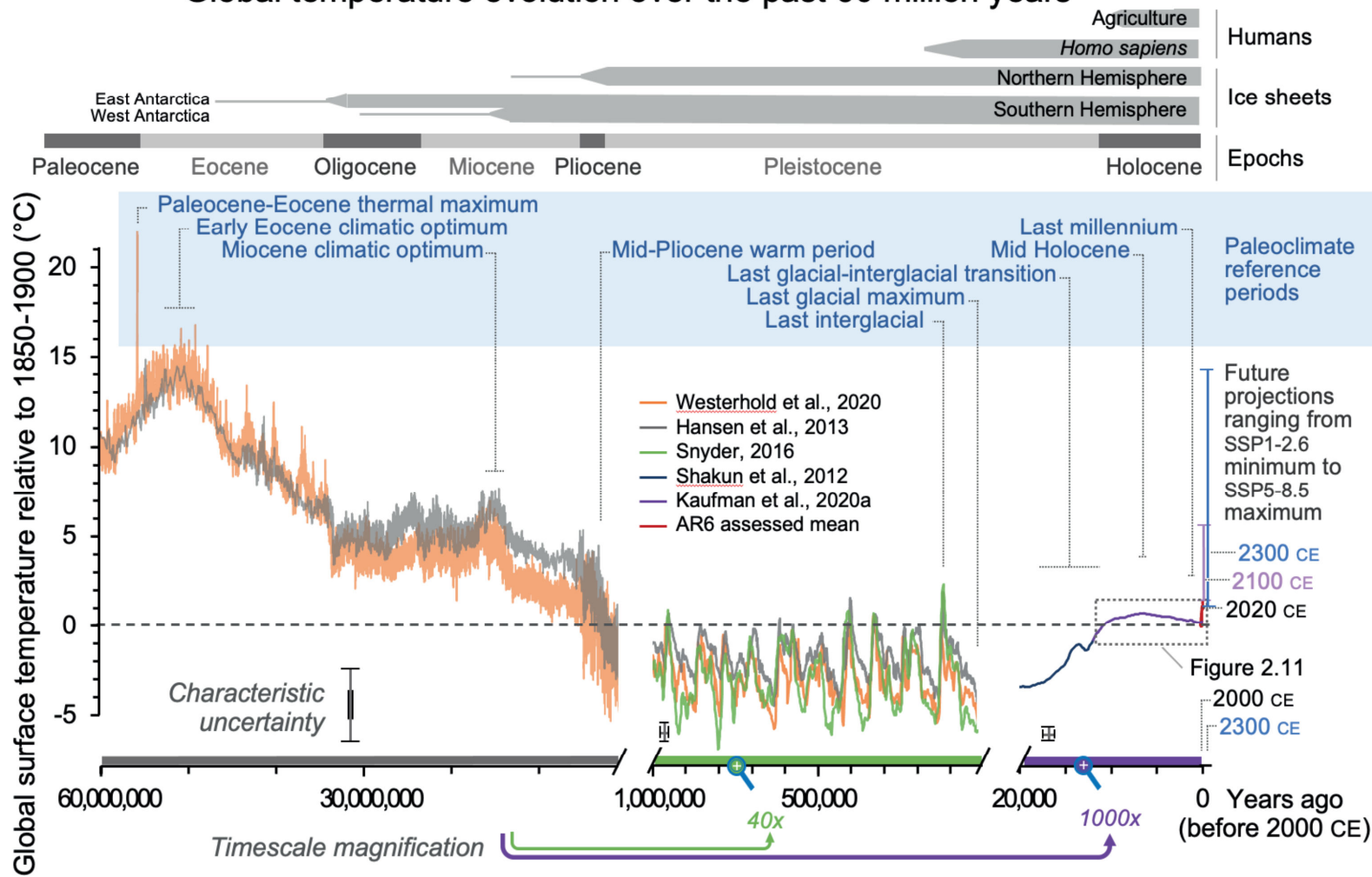
Global mean surface temperature over the past 60 million years



Cross-Chapter Box 2.1, Figure 1 | Global mean surface temperature (GMST) over the past 60 million years (60 Myr) relative to 1850–1900 shown on three time scales. Information about each of the nine paleo reference periods (blue font) and sections in AR6 that discuss these periods are listed in Cross-Chapter Box 2.1 Table 1. Grey horizontal bars at the top mark important events. Characteristic uncertainties are based on expert judgement and are representative of the approximate midpoint of their respective time scales; uncertainties decrease forward in time. GMST estimates for most paleo reference periods (Figure 2.34) overlap with this reconstruction, but take into account multiple lines of evidence. Future projections span the range of global surface air temperature best estimates for SSP1–2.6 and SSP5–8.5 scenarios described in Section 1.6. Range shown for 2100 is based on CMIP6 multi-model mean for 2081–2100 from Table 4.5; range for 2300 is based upon an emulator and taken from Table 4.9. Further details on data sources and processing are available in the chapter data table (Table 2.SM.1).



Global temperature evolution over the past 60 million years



Evolution of atmospheric CO₂

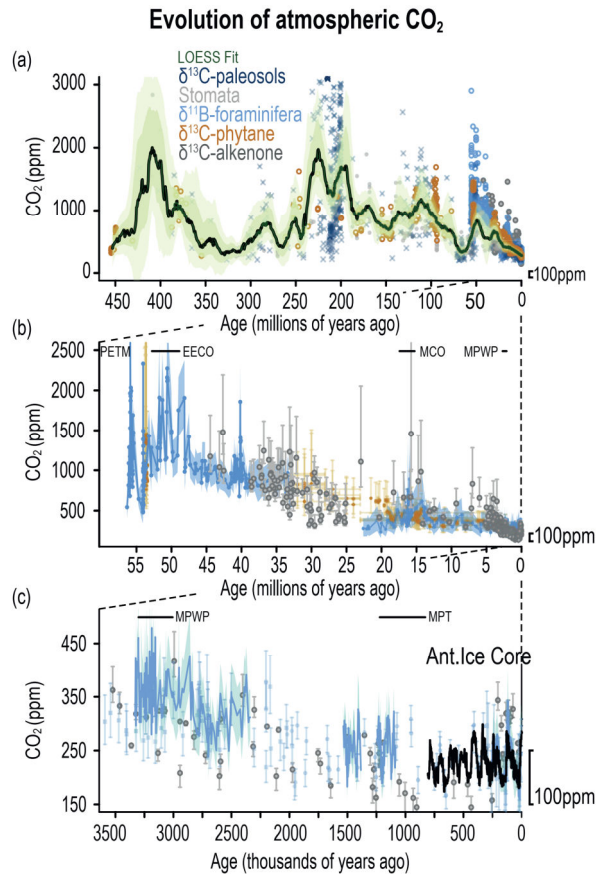
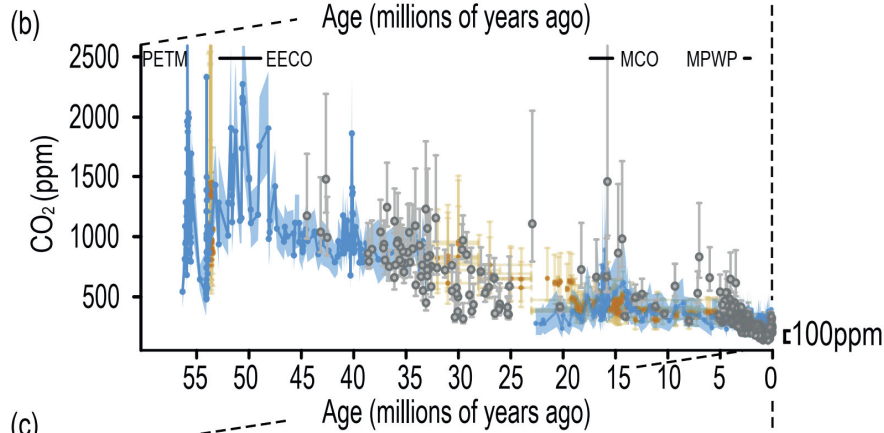
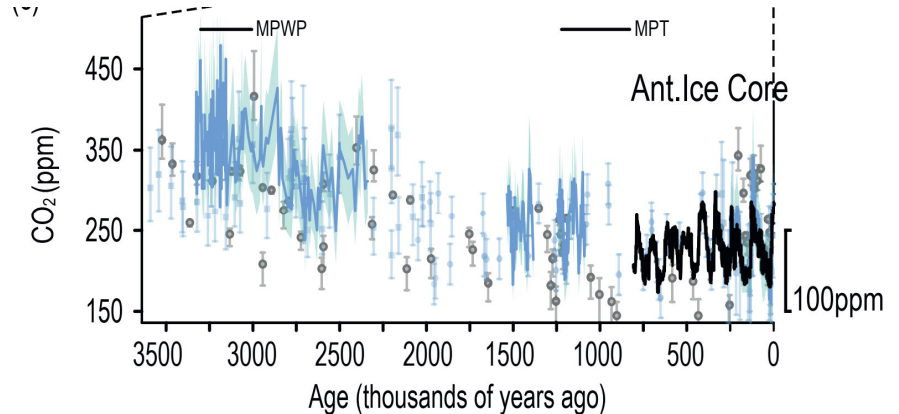
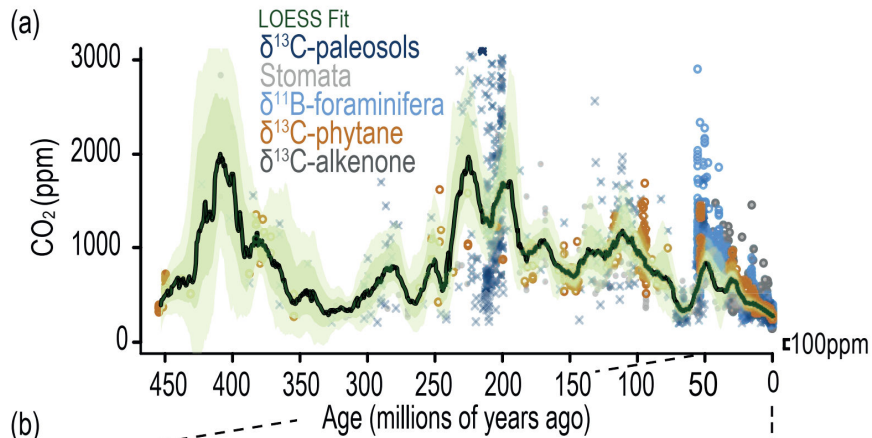


Figure 2.3 | The evolution of atmospheric CO₂ through the last 450 million years (450 Myr). The periods covered are 0–450 Ma **(a)**, 0–58 Ma **(b)**, and 0–3500 ka **(c)**, reconstructed from continental rock, marine sediment and ice core records. Note different time scales and axes ranges in panels (a), (b) and (c). Dark and light green bands in (a) are uncertainty envelopes at 68% and 95% uncertainty, respectively. 100 ppm in each panel is shown by the marker in the lower right-hand corner to aid comparison between panels. In panel (b) and (c) the major paleoclimate reference periods (CCB2.1) have been labelled, and in addition: MPT (Mid Pleistocene Transition), MCO (Miocene Climatic Optimum). Further details on data sources and processing are available in the chapter data table (Table 2.SM.1).



Evolution of atmospheric CO₂

Evolution of atmospheric CO₂



Atmospheric WMGHG concentrations from ice cores

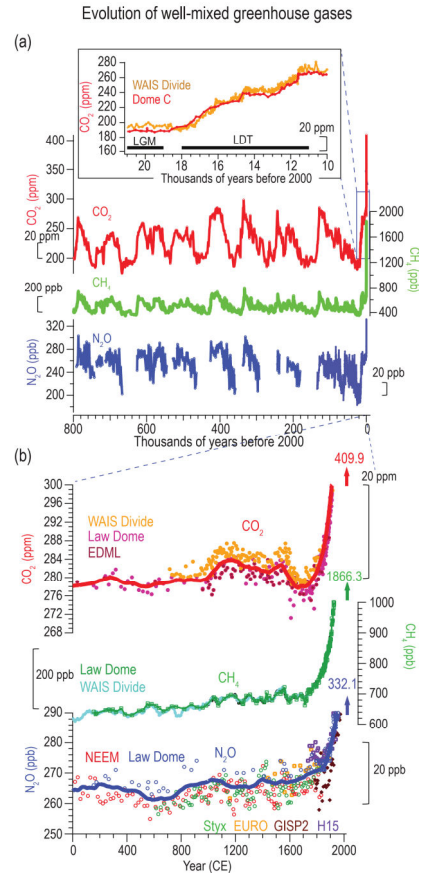
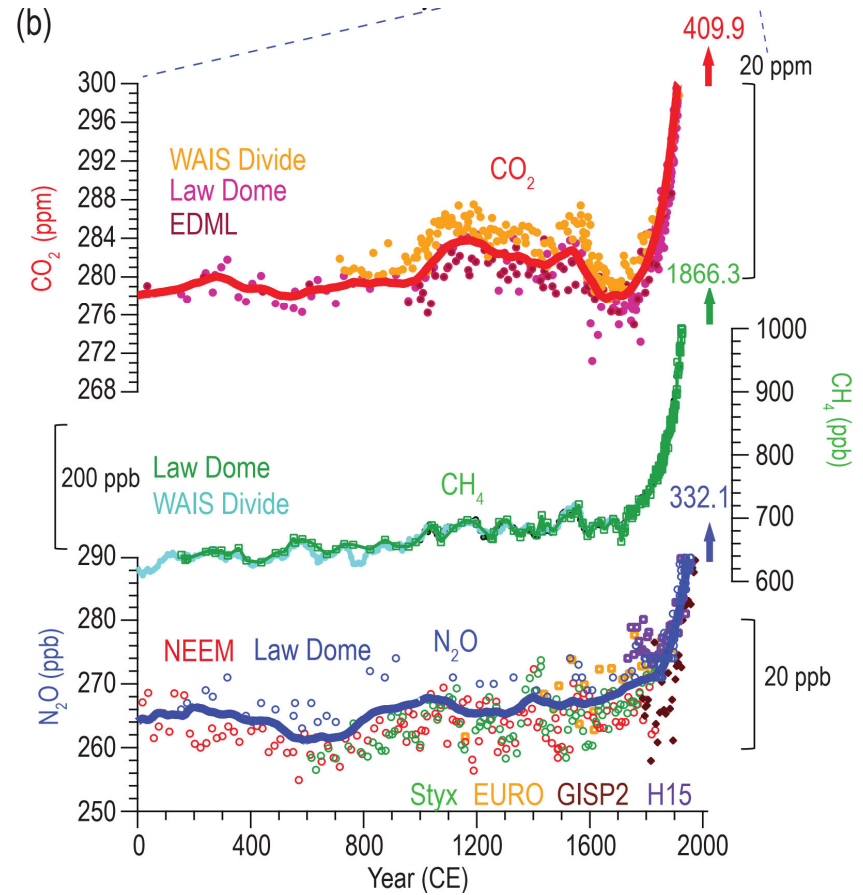
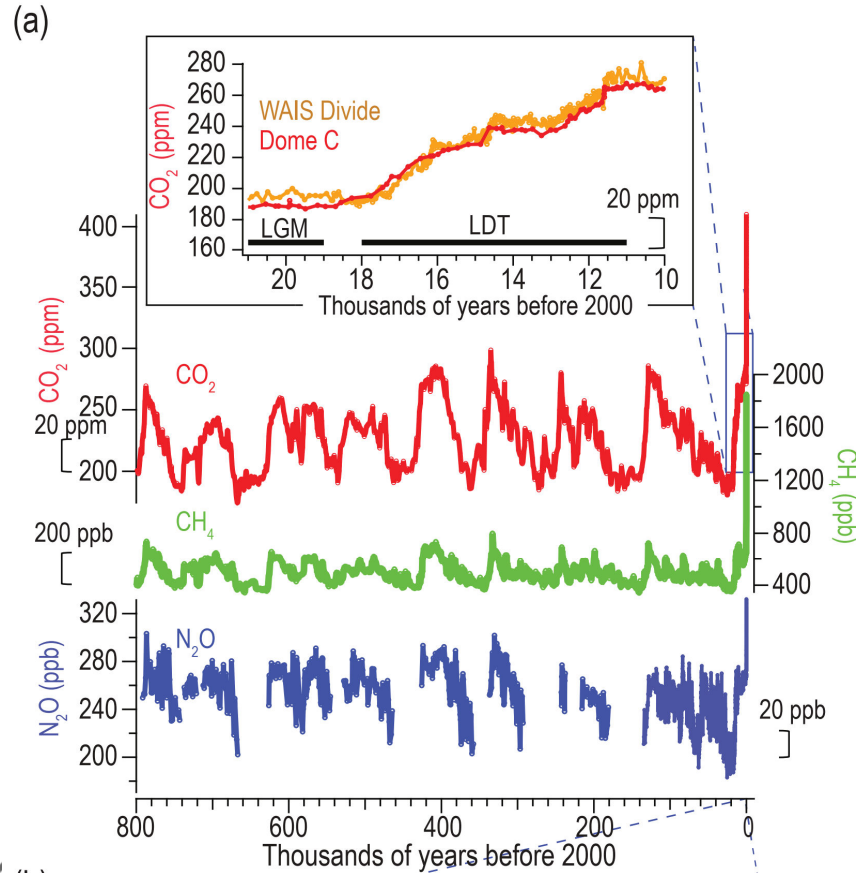


Figure 2.4 | Atmospheric well-mixed greenhouse gas (WMGHG) concentrations from ice cores. (a) Records during the last 800 kyr with the Last Glacial Maximum (LGM) to Holocene transition as inset. **(b)** Multiple high-resolution records over the CE. The horizontal black bars in panel (a) inset indicate LGM and Last Deglacial Termination (LDT) respectively. The red and blue lines in (b) are 100-year running averages for CO₂ and N₂O concentrations, respectively. The numbers with vertical arrows in (b) are instrumentally measured concentrations in 2019. Further details on data sources and processing are available in the chapter data table (Table 2.SM.1).



Atmospheric WMGHG concentrations from ice cores

Evolution of well-mixed greenhouse gases



Globally averaged dry-air mole fractions of greenhouse gases

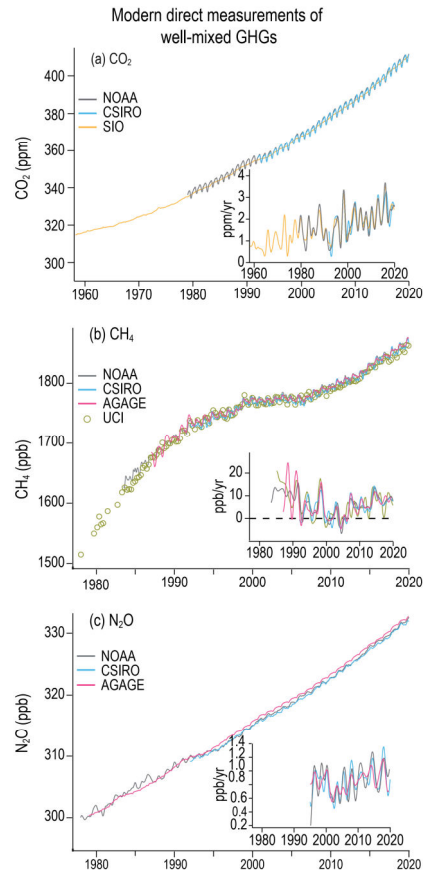
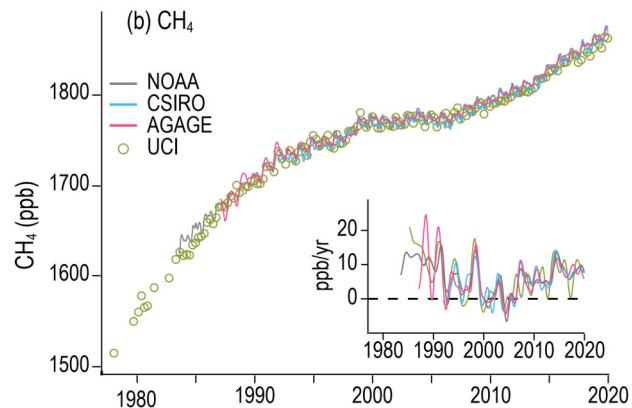
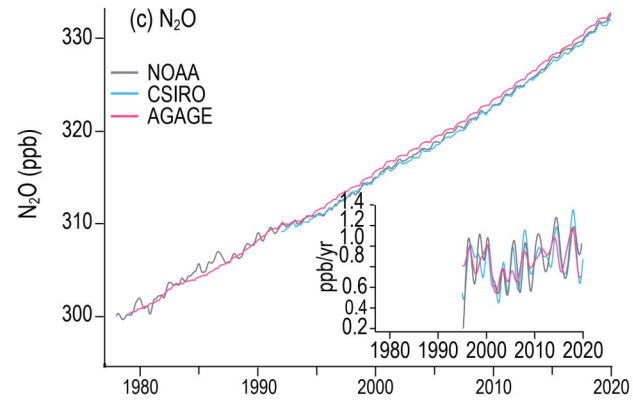
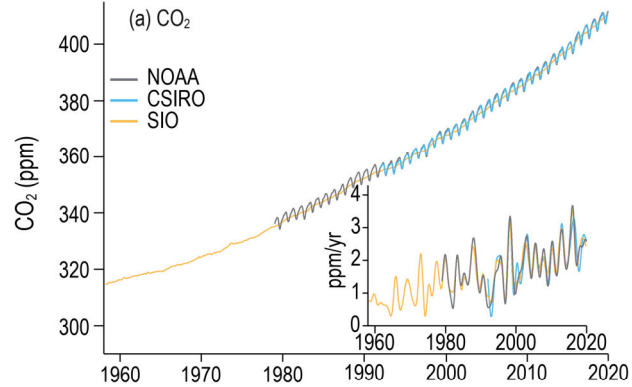


Figure 2.5 | Globally averaged dry-air mole fractions of greenhouse gases. (a) CO₂ from SIO, CSIRO, and NOAA/GML (b) CH₄ from NOAA, AGAGE, CSIRO, and UCI; and (c) N₂O from NOAA, AGAGE, and CSIRO (Table 2.2). Growth rates, calculated as the time derivative of the global means after removing seasonal cycle are shown as inset figures. Note that the CO₂ series is 1958–2019 whereas CH₄, and N₂O are 1979–2019. Units are parts per million (ppm) or parts per billion (ppb). Further details on data are in Annex III, and on data sources and processing are available in the chapter data table (Table 2.SM.1).



Globally averaged dry-air mole fractions of greenhouse gases

Modern direct measurements of well-mixed GHGs



IPCC 2021, Chap. 2



Earth's surface temperature history

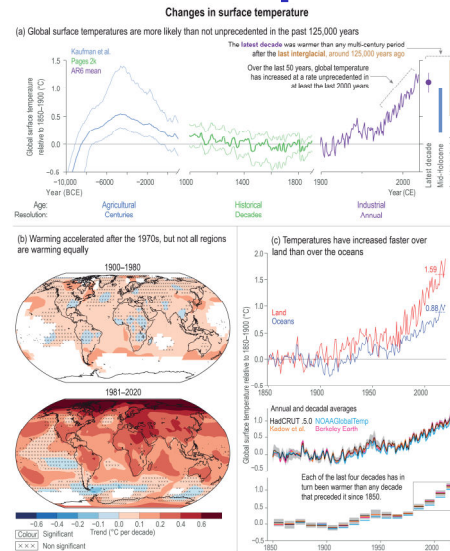
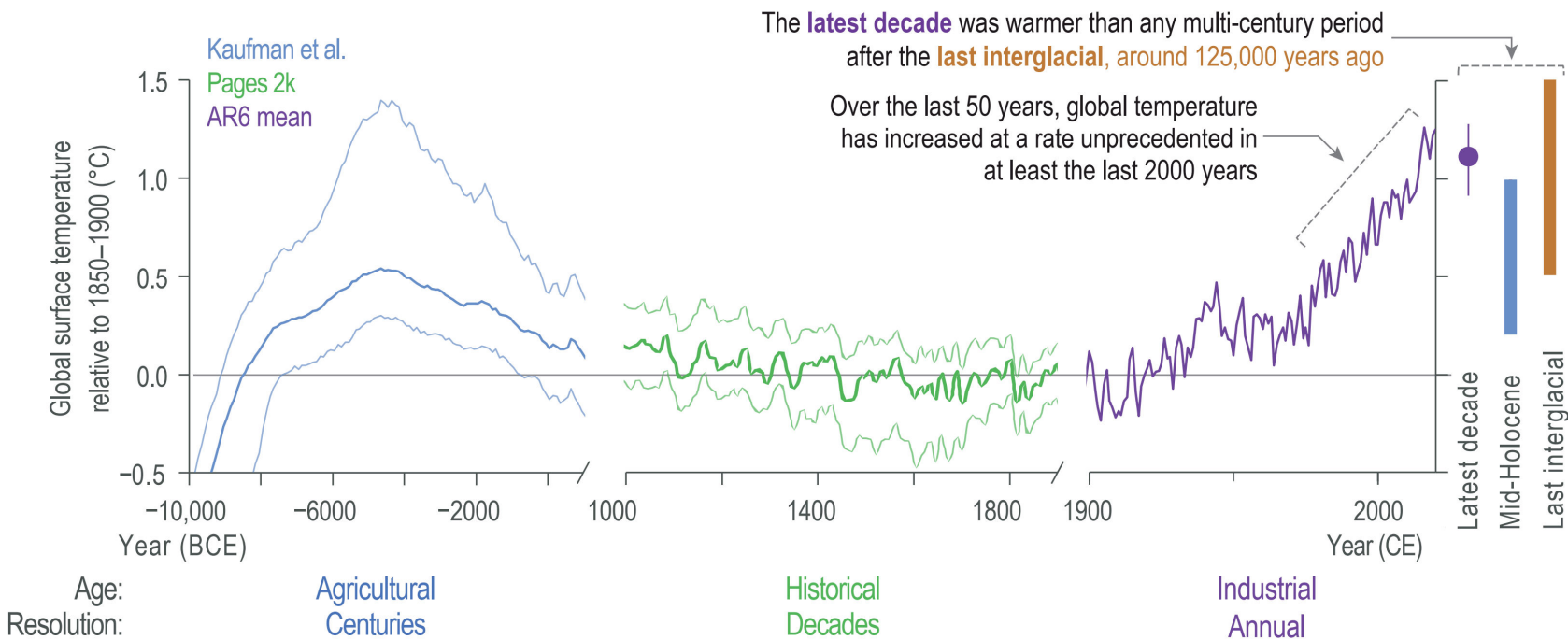


Figure 2.11 | Earth's surface temperature history with key findings annotated within each panel. (a) GMST over the Holocene divided into three time scales: (i) 12 kyr–1 kyr in 100-year time steps; (ii) 1000–1900 CE, 10-year smooth; and (iii) 1900–2020 CE (from panel (c)). Median of the multi-method reconstruction (bold lines), with 5th and 95th percentiles of the ensemble members (thin lines). Vertical bars are the assessed *medium confidence* ranges of GMST for the Last Interglacial and mid-Holocene (Section 2.3.1.1). The last decade value and *very likely* range arises from Section 2.3.1.1.3. **(b)** Spatially resolved trends (°C per decade) for HadCRUTv5 over (upper map) 1900–1980, and (lower map) 1981–2020. Significance is assessed following AR(1) adjustment after Santer et al. (2008), 'x' marks denote non-significant trends. **(c)** Temperature from instrumental data for 1850–2020, including (upper panel) multi-product mean annual time series assessed in Section 2.3.1.1.3 for temperature over the oceans (blue line) and temperature over the land (red line) and indicating the warming to the most recent 10 years; and annually (middle panel) and decadal (bottom panel) resolved averages for the GMST datasets assessed in Section 2.3.1.1.3. The grey shading in each panel shows the uncertainty associated with the HadCRUT5 estimate (Morice et al., 2021). All temperatures relative to the 1850–1900 reference period. Further details on data sources and processing are available in the chapter data table (Table 2.SM.1).

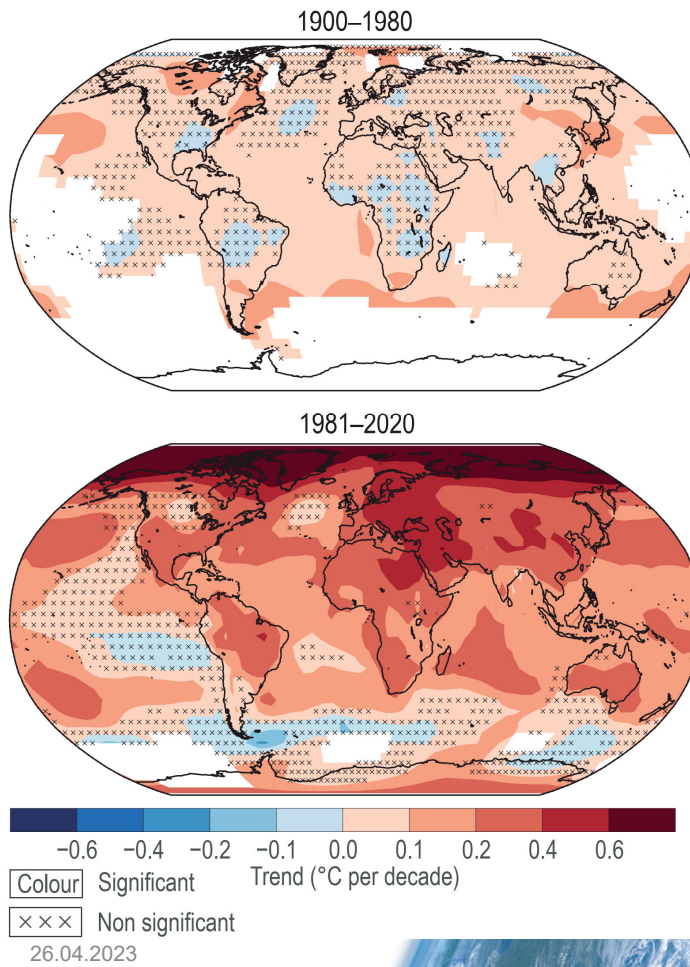
Earth's surface temperature history

Changes in surface temperature

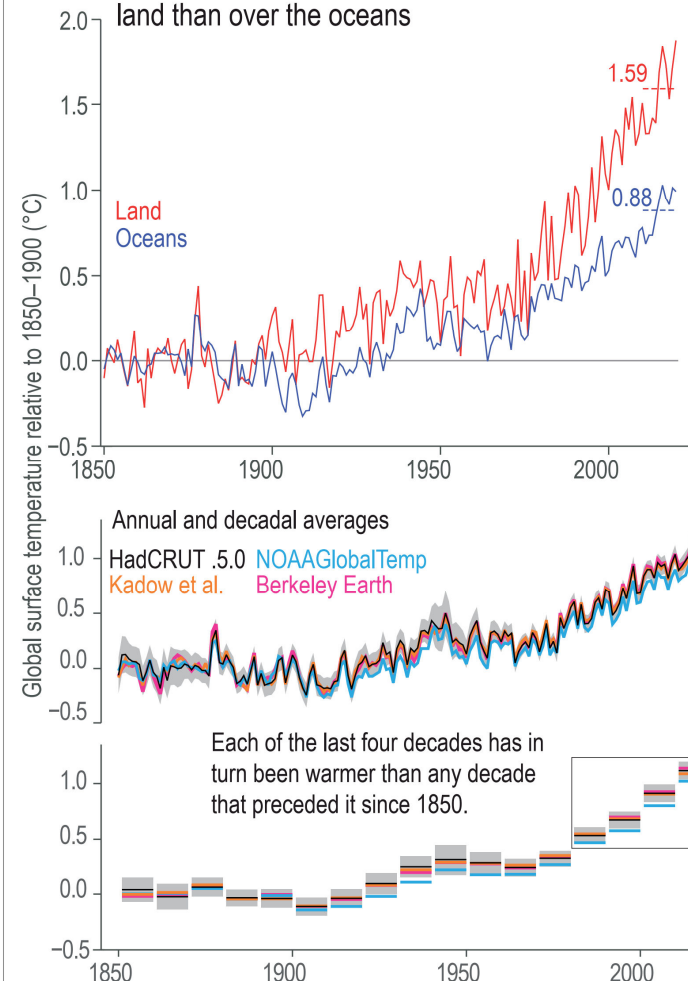
(a) Global surface temperatures are more likely than not unprecedented in the past 125,000 years



(b) Warming accelerated after the 1970s, but not all regions are warming equally



(c) Temperatures have increased faster over land than over the oceans



Klimaänderung I

3. Der Einfluss des Menschen auf das Klimasystem

Robert Sausen

Institut für Physik der Atmosphäre
Deutsches Zentrum für Luft- und Raumfahrt
Oberpfaffenhofen

Vorlesung WS 2022/23

LMU München



Knowledge for Tomorrow

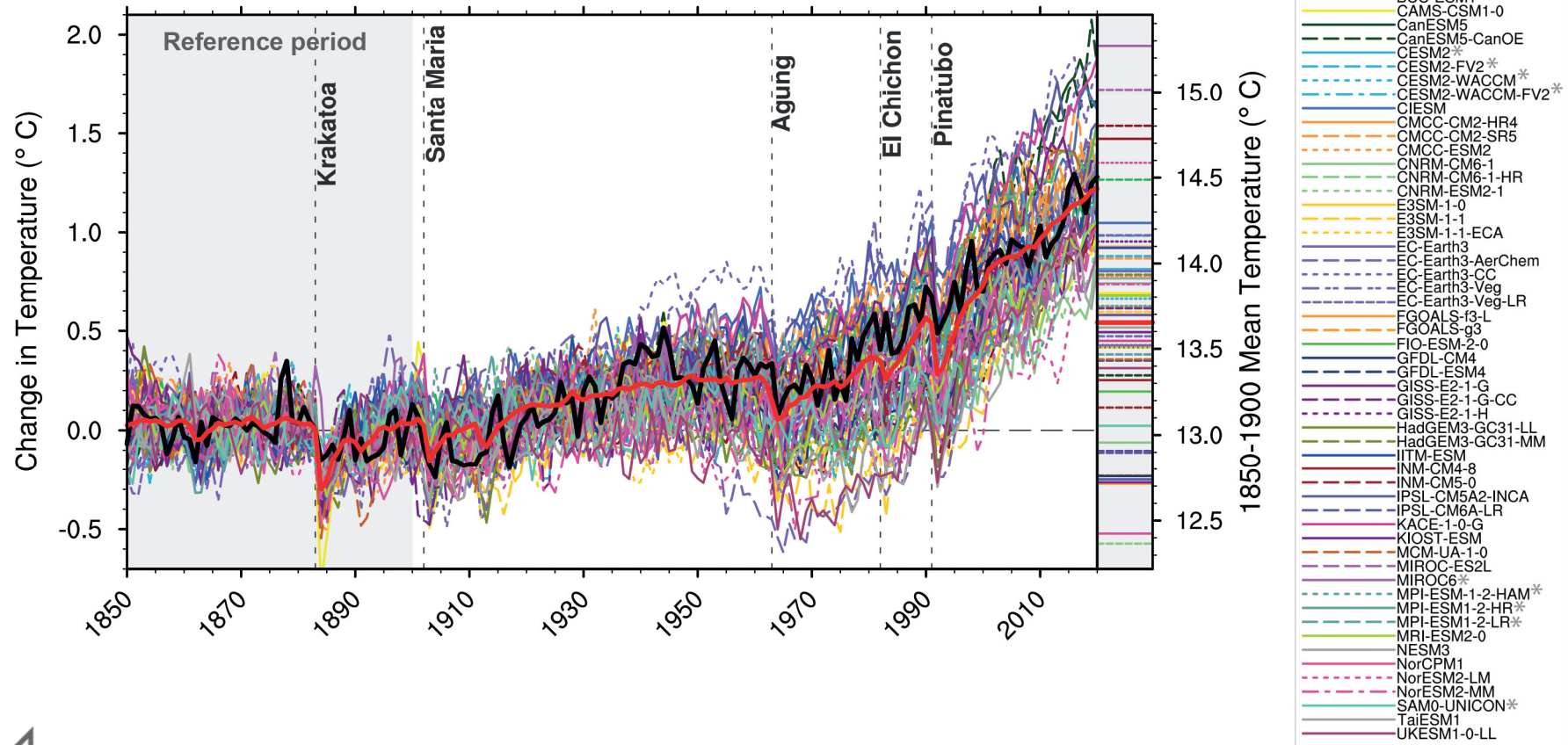
Statements in the Executive Summary

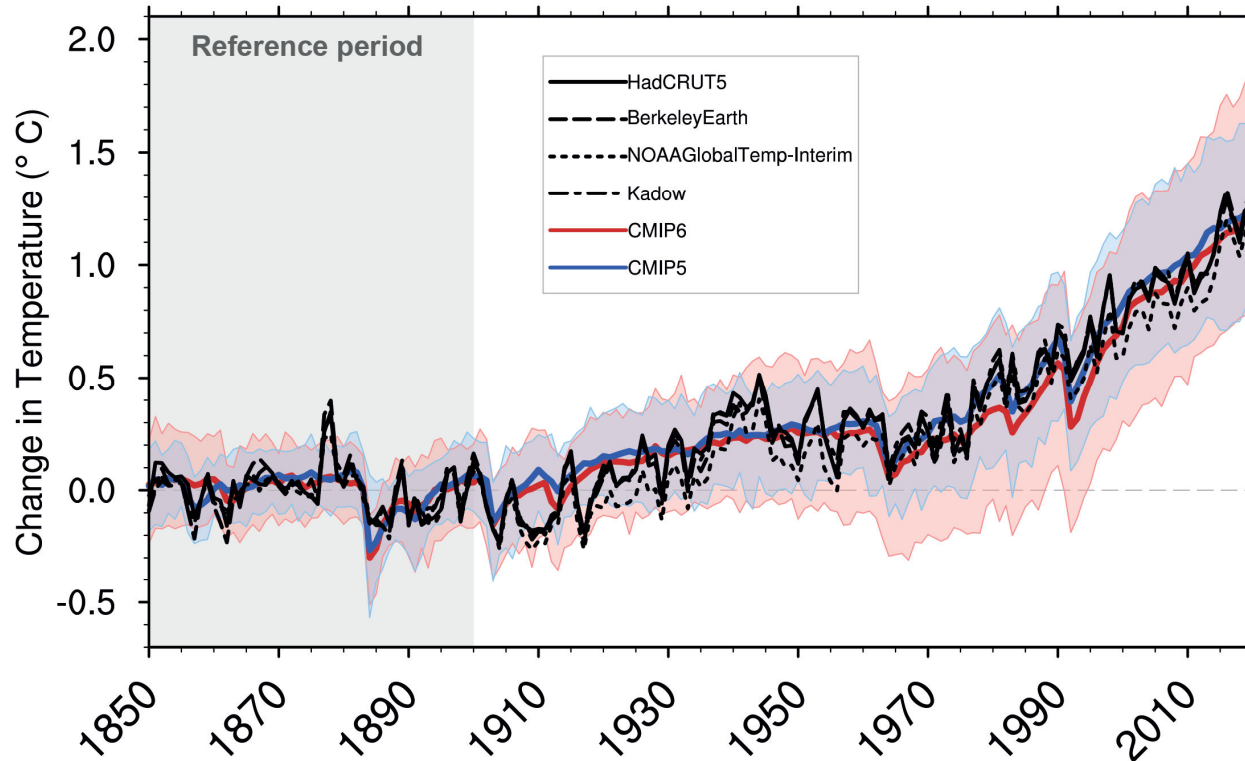
Synthesis across the Climate System (1)

It is unequivocal that human influence has warmed the global climate system since pre-industrial times. Combining the evidence from across the climate system increases the level of confidence in the attribution of observed climate change to human influence and reduces the uncertainties associated with assessments based on single variables. Large-scale indicators of climate change in the atmosphere, ocean, cryosphere and at the land surface show clear responses to human influence consistent with those expected based on model simulations and physical understanding. {3.8.1}



Global mean surface air temperature





- HadCRUT5
- MultiModelMean
- ACCESS-CM2
- ACCESS-ESM1-5
- AWI-CM-1-1-MR
- AWI-ESM-1-1-LR
- BCC-CSM2-MR
- BCC-ESM1
- CAMS-CSM1-0
- CanESM5
- CanESM5-CanOE
- CESM2*
- CESM2-FV2*
- CESM2-WACCM*
- CESM2-WACCM-FV2*
- CIESM
- CMCC-CM2-HR4
- CMCC-CM2-SR5
- CMCC-ESM2
- CNRM-CM6-1
- CNRM-CM6-1-HR
- CNRM-ESM2-1
- ECSM-1-0
- ECSM-1-1
- ECSM-1-1-ECA
- EC-Earth3
- EC-Earth3-AerChem
- EC-Earth3-CC
- EC-Earth3-Veg
- EC-Earth3-Veg-LR
- FGOALS-g3-L
- FGOALS-g3
- FIO-ESM-2-0
- GFDL-CM4
- GFDL-ESM4
- GISS-E2-1-G
- GISS-E2-1-G-CC
- GISS-E2-1-H
- HadGEM3-GC31-LL
- HadGEM3-GC31-MM
- ITM-ESM
- INM-CM4-8
- INM-CM5-0
- IPSL-CM5A2-INCA
- IPSL-CM6A-LR
- KACE-1-0-G
- KIOST-ESM
- MCM-UA-1-0
- MIROC-ES2L
- MIROC6*
- MPI-ESM-1-2-HAM*
- MPI-ESM1-2-HR*
- MPI-ESM1-2-LR*
- MRI-ESM2-0
- NESM3
- NorCPM1
- NorESM2-LM
- NorESM2-MM
- SAM0-UNICON*
- TaiESM1
- UKESM1-0-LL



Assessed contributions to observed warming, and supporting lines of evidence

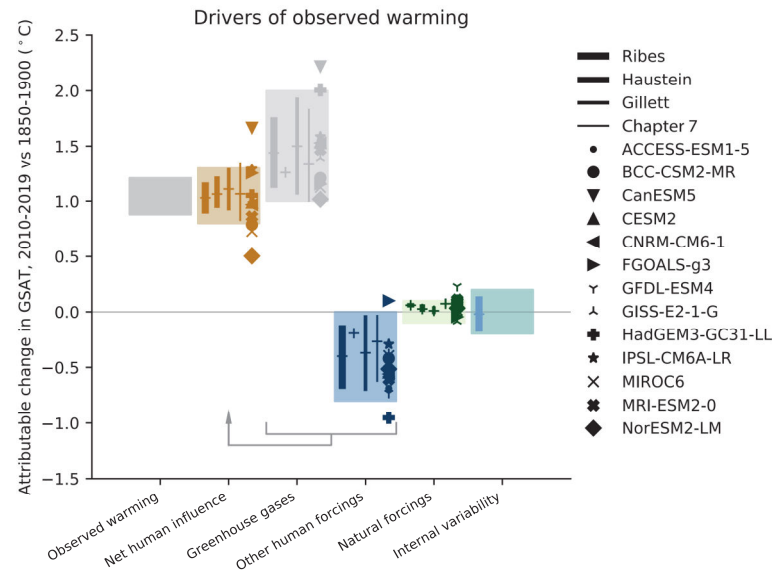
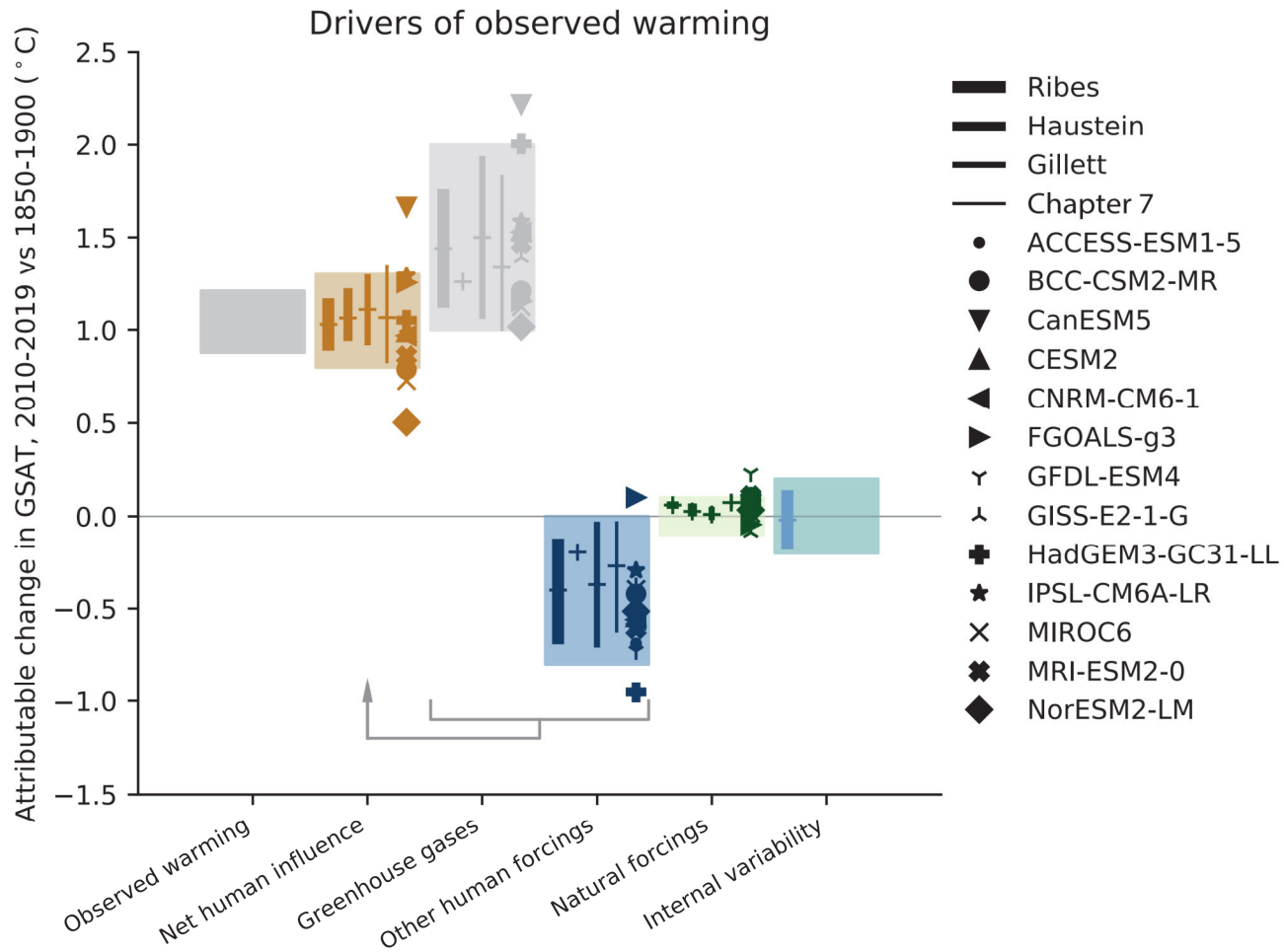


Figure 3.8 | Assessed contributions to observed warming, and supporting lines of evidence. Shaded bands show assessed *likely* ranges of temperature change in GSAT, 2010–2019 relative to 1850–1900, attributable to net human influence, well-mixed greenhouse gases, other human forcings (aerosols, ozone, and land-use change), natural forcings, and internal variability, and the 5–95% range of observed warming. Bars show 5–95% ranges based on (left to right) Haustein et al. (2017), Gillett et al. (2021) and Ribes et al. (2021), and crosses show the associated best estimates. No 5–95% ranges were provided for the Haustein et al. (2017) greenhouse gas or other human forcings contributions. The Ribes et al. (2021) results were updated using a revised natural forcing time series, and the Haustein et al. (2017) results were updated using HadCRUT5. The Chapter 7 best estimates and ranges were derived using assessed forcing time series and a two-layer energy balance model as described in Section 7.3.5.3. Coloured symbols show the simulated responses to the forcings concerned in each of the models indicated. Further details on data sources and processing are available in the chapter data table (Table 3.SM.1).





Global, land, ocean and continental annual mean near-surface air temperatures anomalies in CMIP6 models and observations

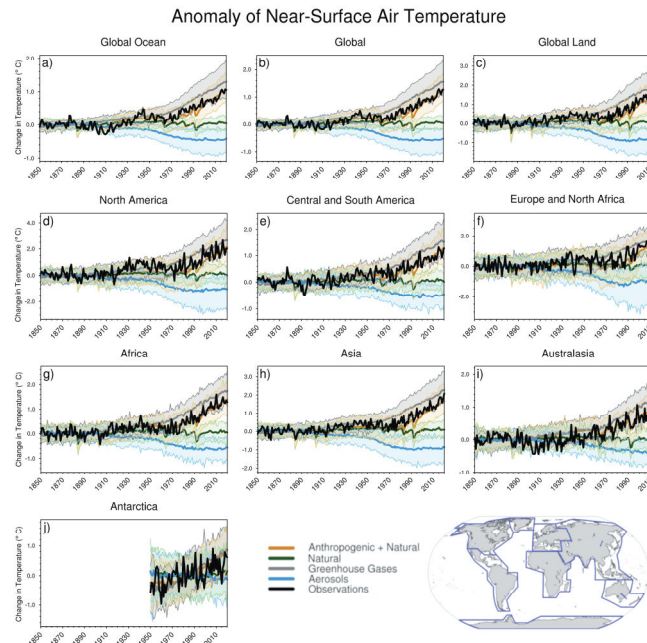
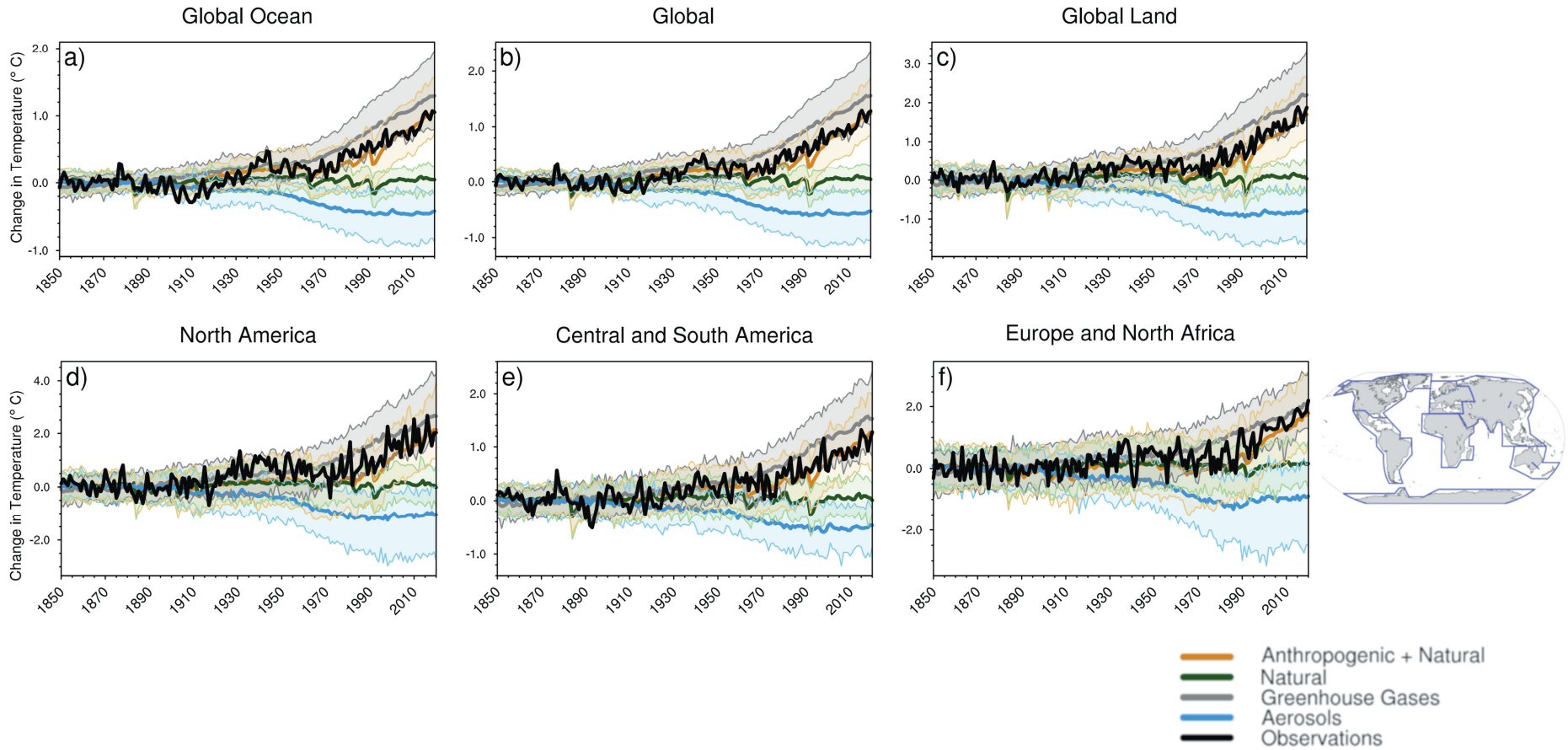
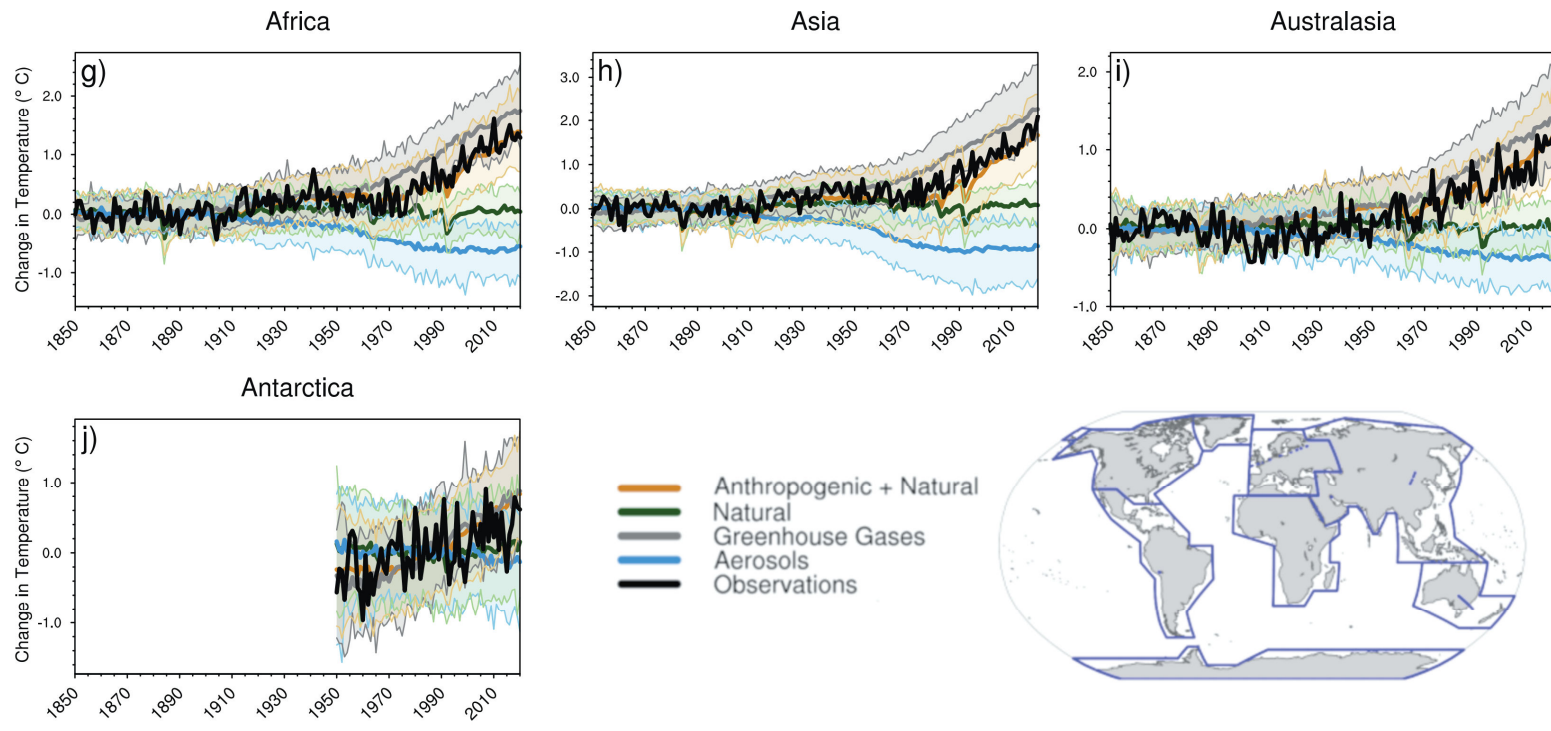


Figure 3.9 | Global, land, ocean and continental annual mean near-surface air temperatures anomalies in CMIP6 models and observations. Time series are shown for CMIP6 historical anthropogenic and natural (brown), natural-only (green), greenhouse gas only (grey) and aerosol only (blue) simulations (thick lines show multi-model means and shaded regions show the 5th to 95th percentile ranges) and for HadCRUT5 (black). All models have been subsampled using the HadCRUT5 observational data mask. Temperature anomalies are shown relative to 1950–2010 for Antarctica and relative to 1850–1900 for other continents. CMIP6 historical simulations are extended using the SSP2-4.5 scenario simulations. All available ensemble members were used (see Section 3.2). Regions are defined by Iturbide et al. (2020). Further details on data sources and processing are available in the chapter data table (Table 3.SM.1).



Anomaly of Near-Surface Air Temperature





Global ocean heat content in CMIP6 simulations and observations

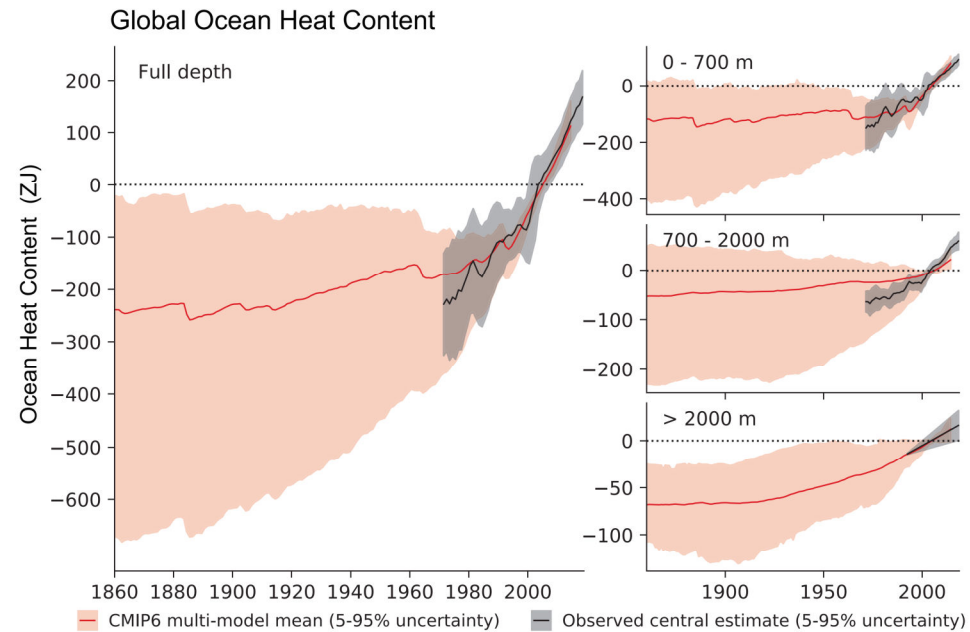
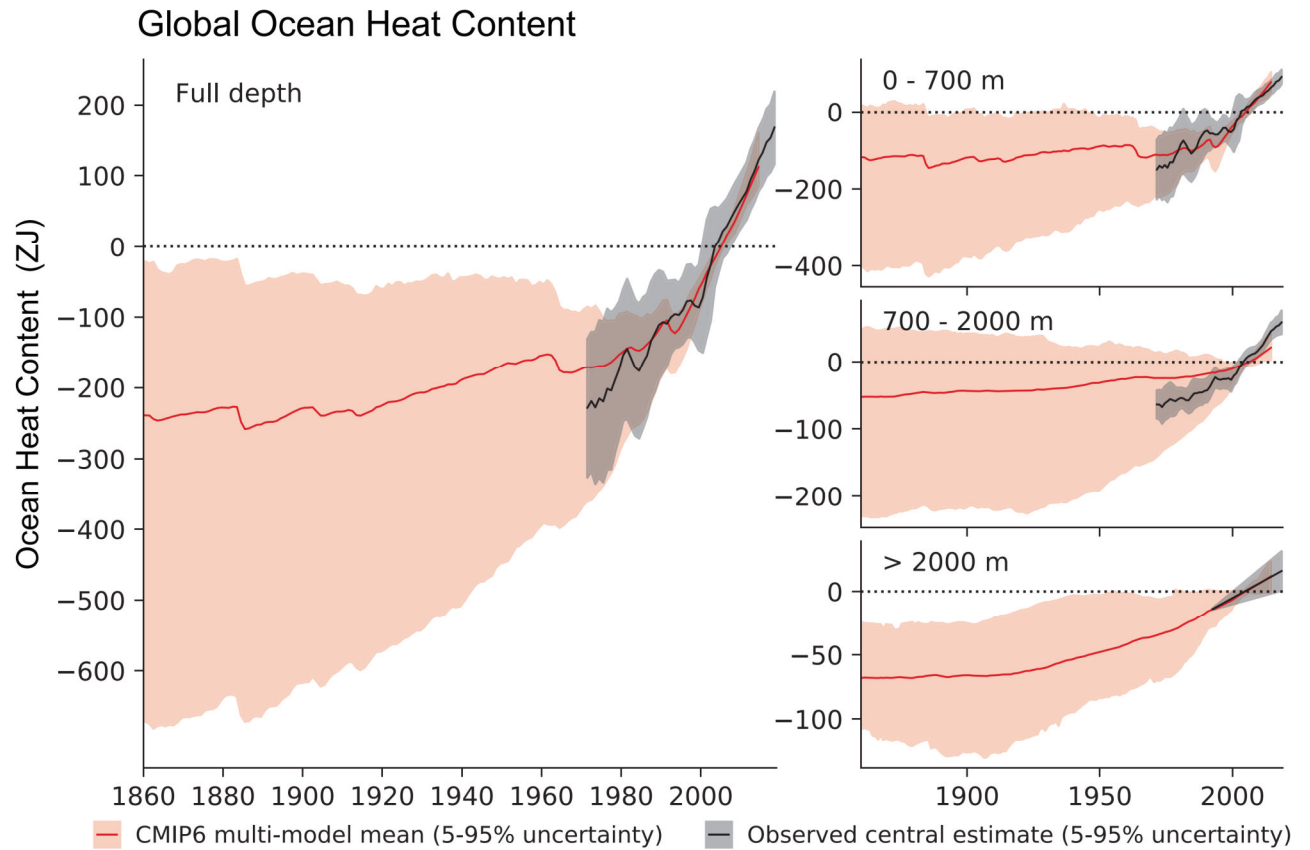


Figure 3.26 | Global ocean heat content in CMIP6 simulations and observations. Time series of observed (black) and simulated (red) global ocean heat content anomalies with respect to 1995–2014 for the full ocean depth (**left-hand panel**); upper layer: 0–700 m (**top right-hand panel**); intermediate layer: 700–2000 m (**middle right-hand panel**); and the abyssal ocean: >2000 m (**bottom right-hand panel**). The best estimate observations (black solid line) for the period of 1971–2018, along with *very likely* ranges (black shading) are from Section 2.3.3.1. For the models (1860–2014), ensemble members from 15 CMIP6 models are used to calculate the multi-model mean values (red solid line) after averaging across simulations for each independent model. The *very likely* ranges in the simulations are shown in red shading. Simulation drift has been removed from all CMIP6 historical runs using a contemporaneous portion of the linear fit to each corresponding pre-industrial control run (Gleckler et al., 2012). Units are zettajoules (ZJ; 10^{21} joule). Further details on data sources and processing are available in the chapter data table (Table 3.SM.1).

1 ZJ = 10^{21} J
 $\approx 2.78 \cdot 10^{11}$ kWh = 278 PWh

PV-Anlage Sausen: ~ 3.5 MWh

Windkraftanlage Berg:
 ~ 21 GWh (2021, 4 Turbinen)



Summary figure showing simulated and observed changes in key large-scale indicators of climate change across the climate system

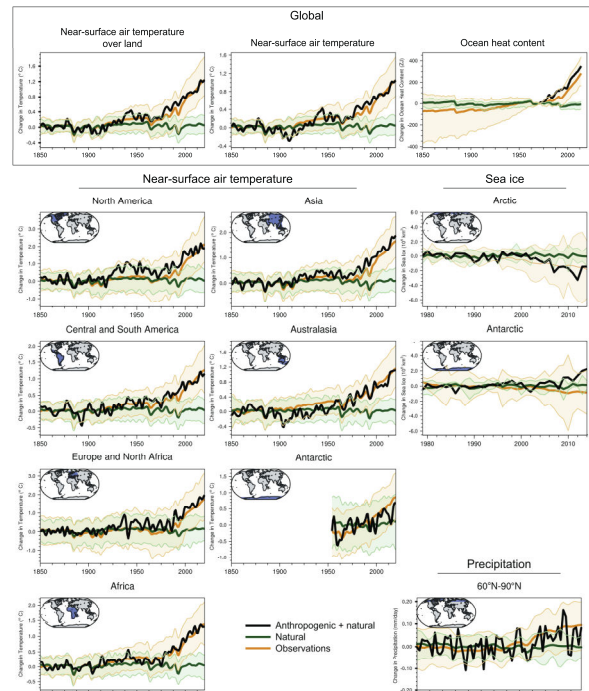
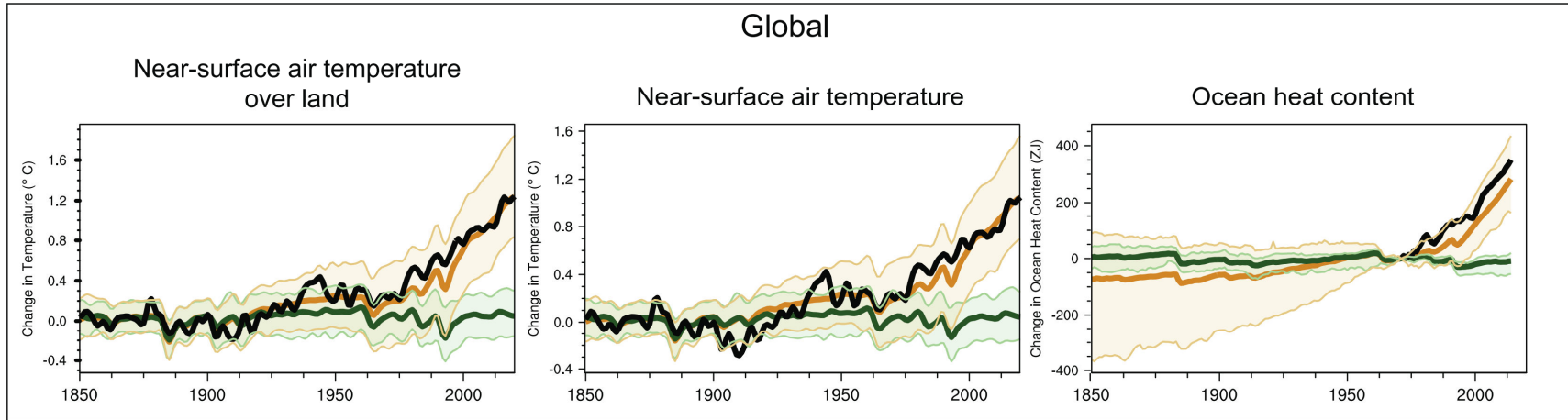
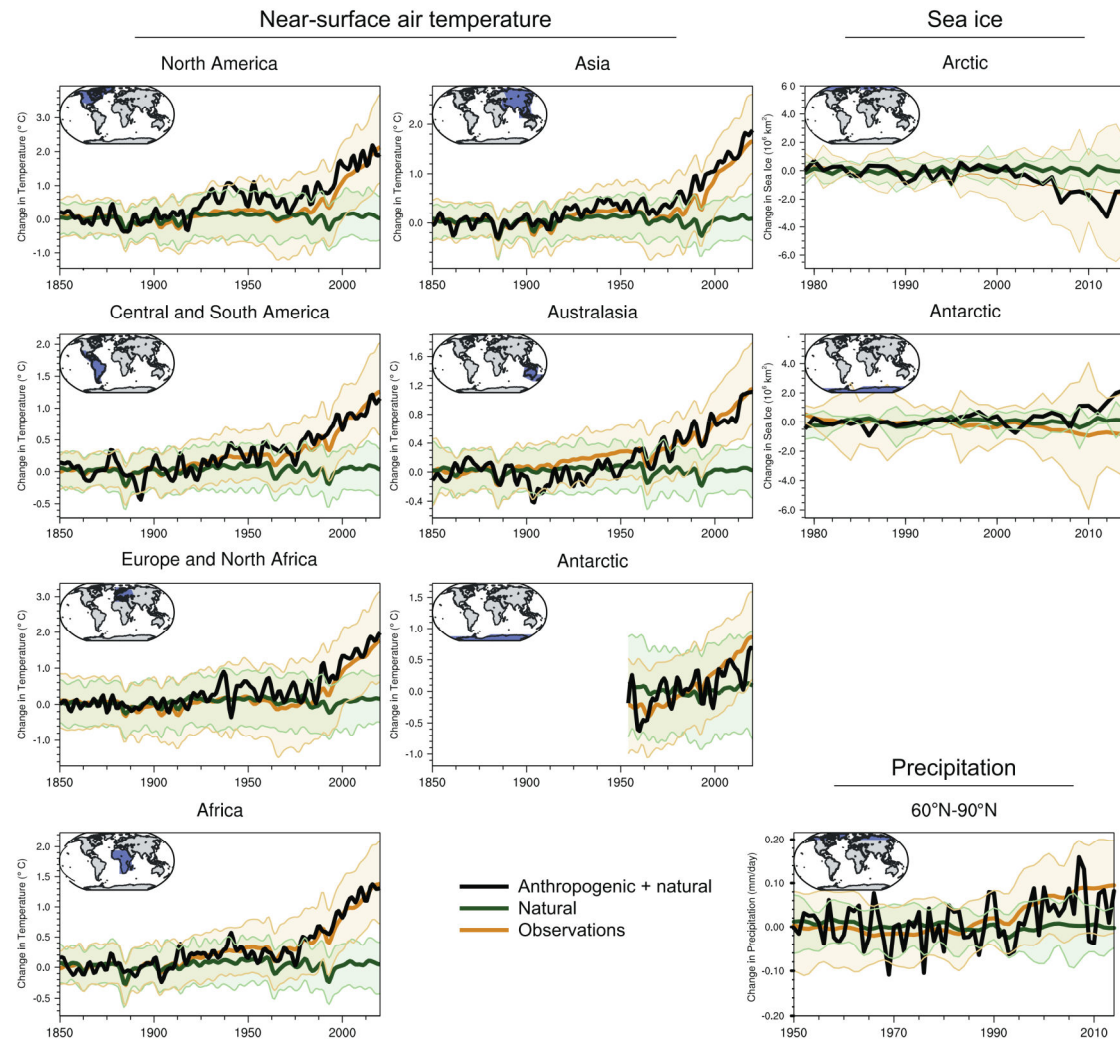


Figure 3.41 | Summary figure showing simulated and observed changes in key large-scale indicators of climate change across the climate system, for continental, ocean basin and larger scales. Black lines show observations, brown lines and shading show the multi-model mean and 5th–95th percentile ranges for CMIP6 historical simulations including anthropogenic and natural forcing, and blue lines and shading show corresponding ensemble means and 5th–95th percentile ranges for CMIP6 natural-only simulations. Temperature time series are as in Figure 3.9, but with smoothing using a low pass filter. Precipitation time series are as in Figure 3.15 and ocean heat content as in Figure 3.26. Further details on data sources and processing are available in the chapter data table (Table 3.SM.1).





Klimaänderung I

4. Das zukünftige globale Klima: Szenarien-basierte Projektionen und kurzfristiger Ausblick

Robert Sausen

Institut für Physik der Atmosphäre
Deutsches Zentrum für Luft- und Raumfahrt
Oberpfaffenhofen

Vorlesung WS 2021/22

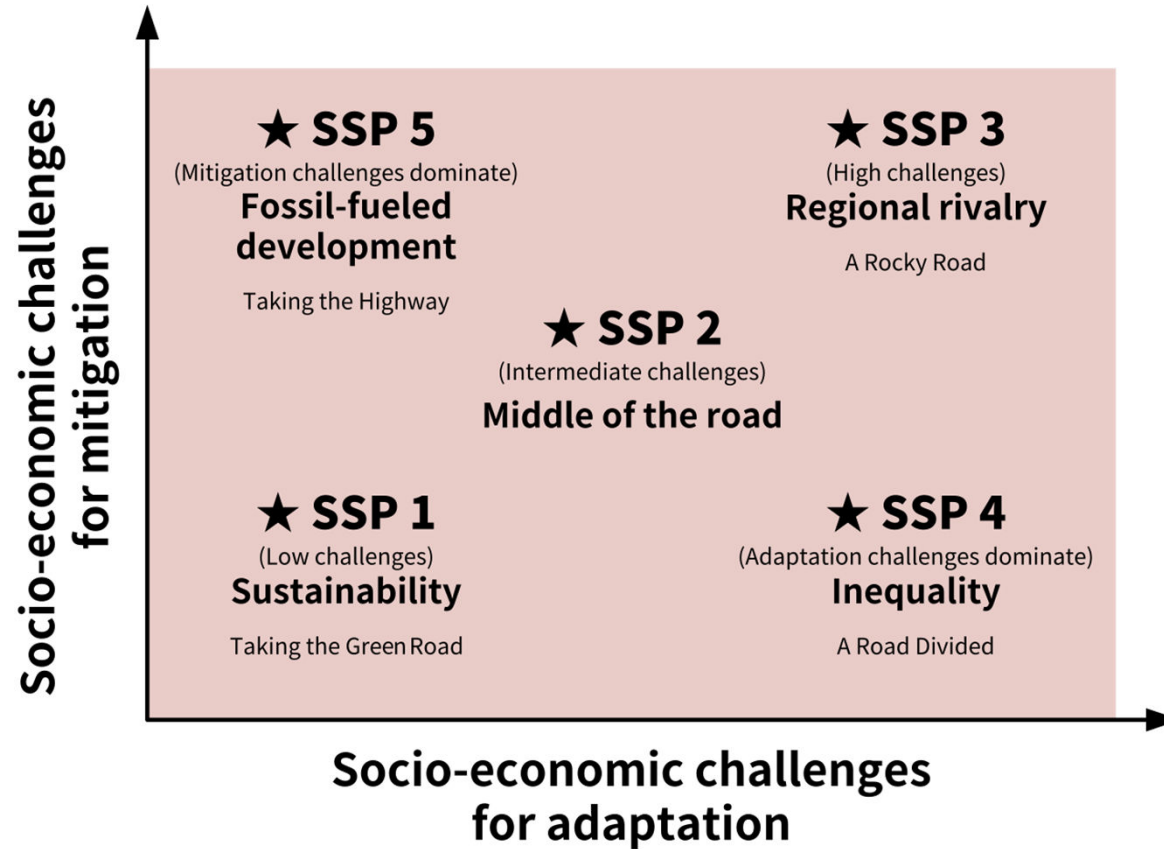
LMU München



Knowledge for Tomorrow

Die SSP-Szenarien

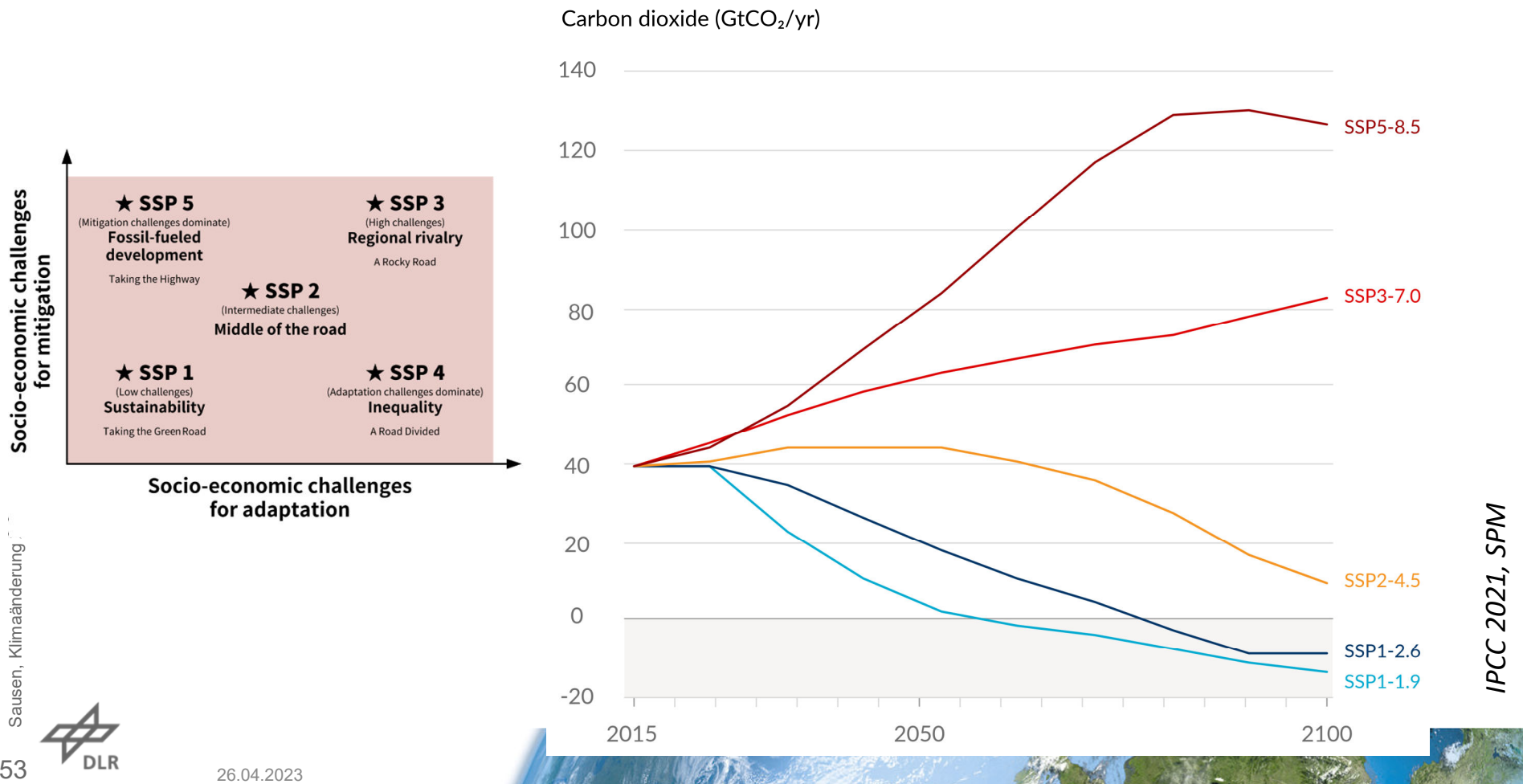
Shared Socioeconomic Pathways



<https://en.wikipedia.org>



Die SSP-Szenarien – Shared Socioeconomic Pathways



Selected indicators of global climate change from CMIP6 historical and scenario simulations

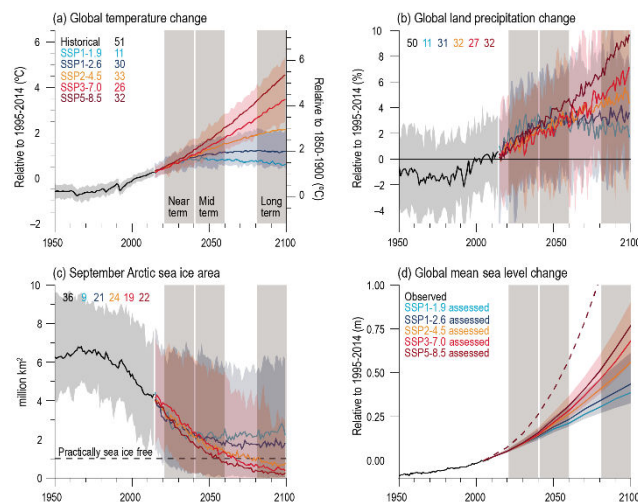
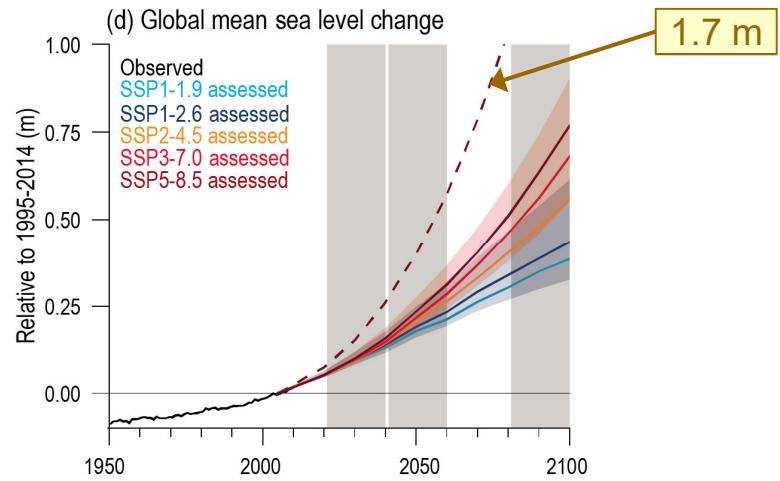
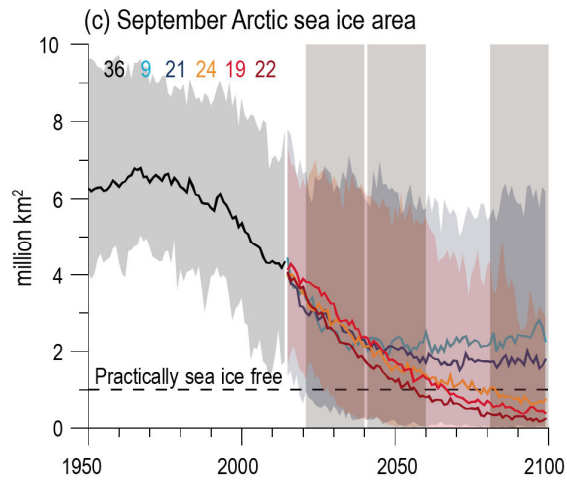
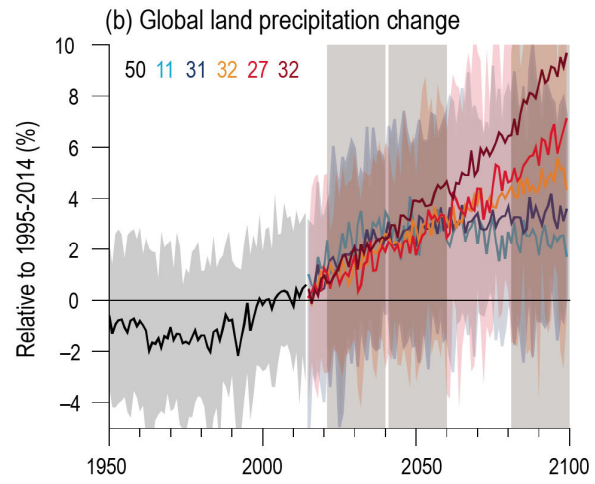
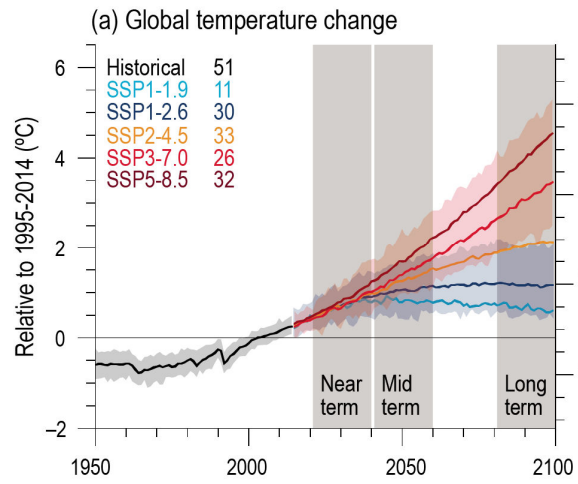


Figure 4.2 | Selected indicators of global climate change from CMIP6 historical and scenario simulations. (a) Global surface air temperature changes relative to the 1995–2014 average (left axis) and relative to the 1850–1900 average (right axis; offset by 0.82°C, which is the multi-model mean and close to observed best estimate, Cross-Chapter Box 2.1, Table 1). (b) Global land precipitation changes relative to the 1995–2014 average. (c) September Arctic sea ice area. (d) Global mean sea level (GMSL) change relative to the 1995–2014 average. (a), (b) and (d) are annual averages, (c) are September averages. In (a–c), the curves show averages over the CMIP6 simulations, the shadings around the SSP1-2.6 and SSP3-7.0 curves show 5–95% ranges, and the numbers near the top show the number of model simulations used. Results are derived from concentration-driven simulations. In (d), the barystatic contribution to GMSL (i.e., the contribution from land-ice melt) has been added offline to the CMIP6 simulated contributions from thermal expansion (thermohaline). The shadings around the SSP1-2.6 and SSP3-7.0 curves show 5–95% ranges. The dashed curve is the *low confidence* and low likelihood outcome at the high end of SSP5-8.5 and reflects deep uncertainties arising from potential ice-sheet and ice-cliff instabilities. This curve at year 2100 indicates 1.7 m of GMSL rise relative to 1995–2014. More information on the calculation of GMSL is available in Chapter 9, and further regional details are provided in the Atlas. Further details on data sources and processing are available in the chapter data table (Table 4.SM.1).



Mid- and long-term change of annual mean surface temperature

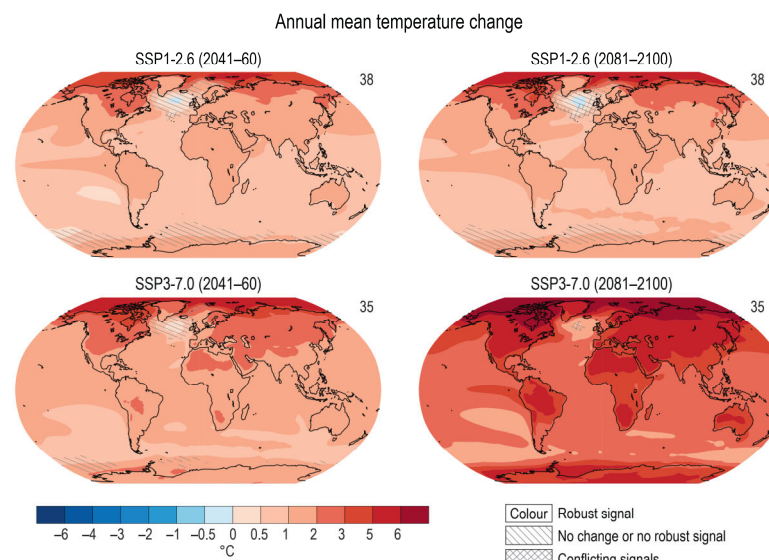
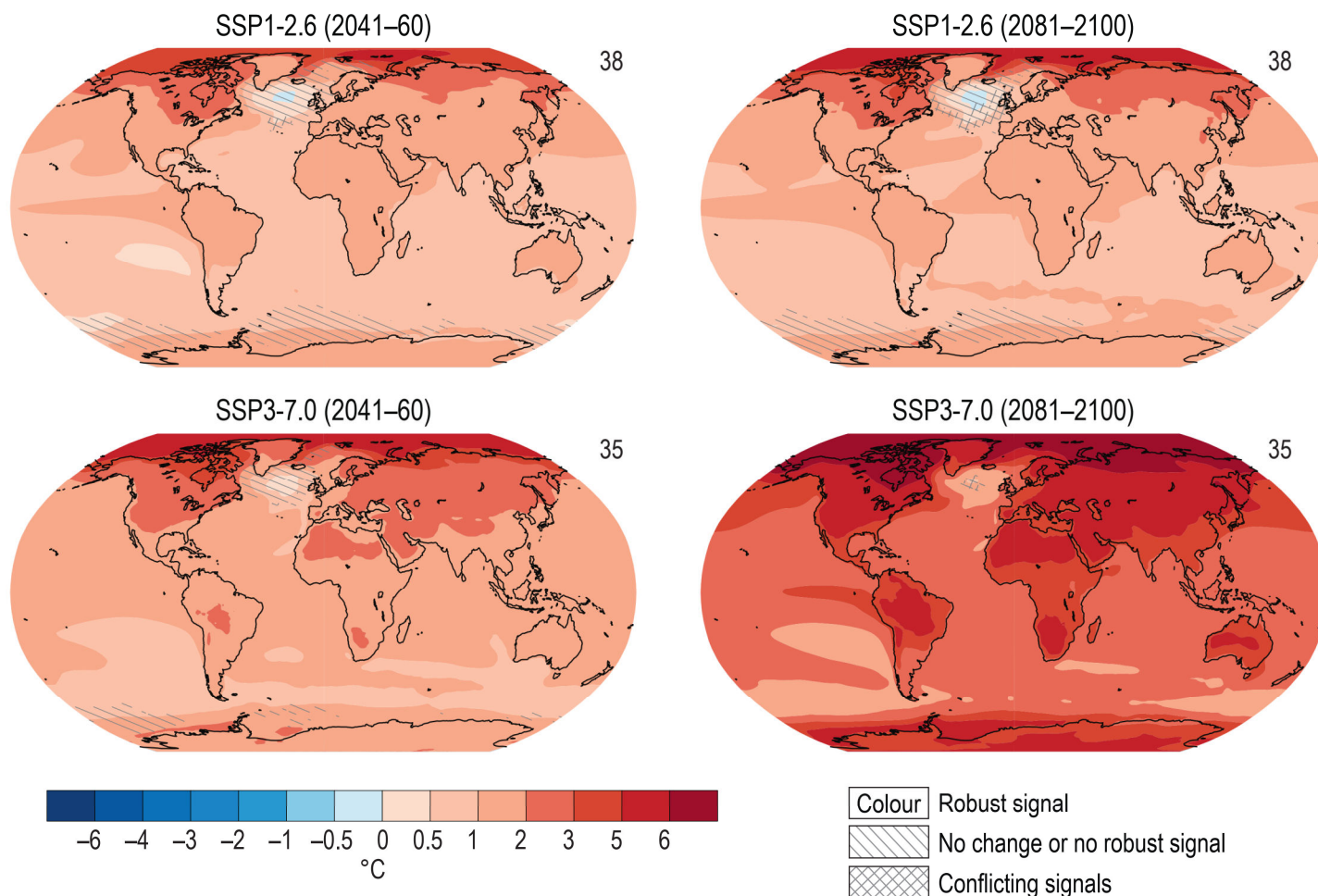


Figure 4.19 | Mid- and long-term change of annual mean surface temperature. Displayed are projected spatial patterns of multi-model mean change in annual mean near-surface air temperature (°C) in 2041–2060 and 2081–2100 relative to 1995–2014 for **(top)** SSP1-2.6 and **(bottom)** SSP3-7.0. The number of models used is indicated in the top right of the maps. No overlay indicates regions where the change is robust and *likely* emerges from internal variability, that is, where at least 66% of the models show a change greater than the internal-variability threshold (see Section 4.2.6) and at least 80% of the models agree on the sign of change. Diagonal lines indicate regions with no change or no robust significant change, where fewer than 66% of the models show change greater than the internal-variability threshold. Crossed lines indicate areas of conflicting signals where at least 66% of the models show change greater than the internal-variability threshold but fewer than 80% of all models agree on the sign of change. Further details on data sources and processing are available in the chapter data table (Table 4.SM.1).

Annual mean temperature change



Projected spatial patterns of change in annual average near-surface temperature (°C) at different levels of global warming.

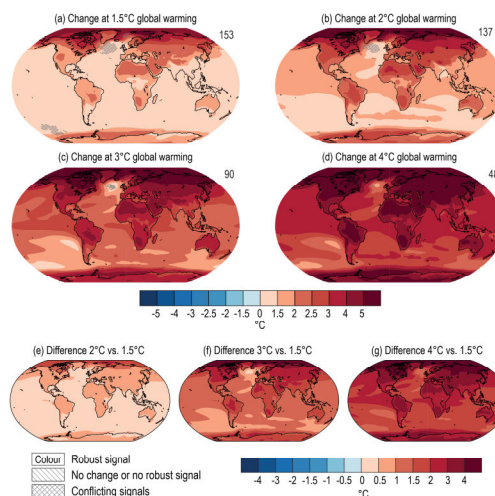
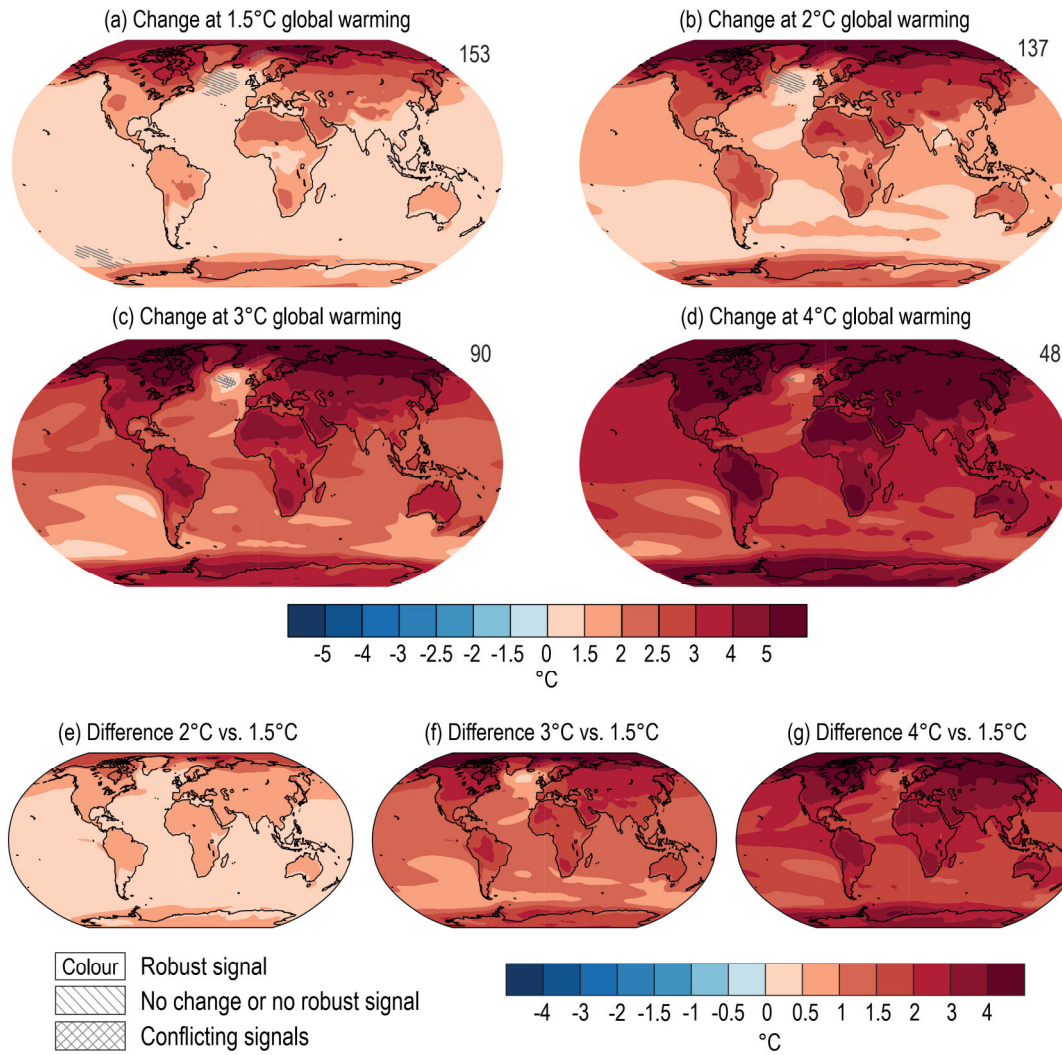


Figure 4.31 | Projected spatial patterns of change in annual average near-surface temperature (°C) at different levels of global warming. Displayed are **(a–d)** spatial patterns of change in annual average near-surface temperature at 1.5°C, 2°C, 3°C, and 4°C of global warming relative to the period 1850–1900 and **(e–g)** spatial patterns of differences in temperature change at 2°C, 3°C, and 4°C of global warming compared to 1.5°C of global warming. The number of models used is indicated in the top right of the maps. No overlay indicates regions where the change is robust and *likely* emerges from internal variability. That is, where at least 66% of the models show a change greater than the internal-variability threshold (Section 4.2.6) and at least 80% of the models agree on the sign of change. Diagonal lines indicate regions with no change or no robust significant change, where fewer than 66% of the models show change greater than the internal-variability threshold. Crossed lines indicate areas of conflicting signals where at least 66% of the models show change greater than the internal-variability threshold but fewer than 80% of all models agree on the sign of change. Values were assessed from a 20-year period at a given warming level, based on model simulations under the Tier-1 SSPs of CMIP6. Further details on data sources and processing are available in the chapter data table (Table 4.SM.1).



26.04.2023



Long-term change of annual and zonal mean atmospheric temperature

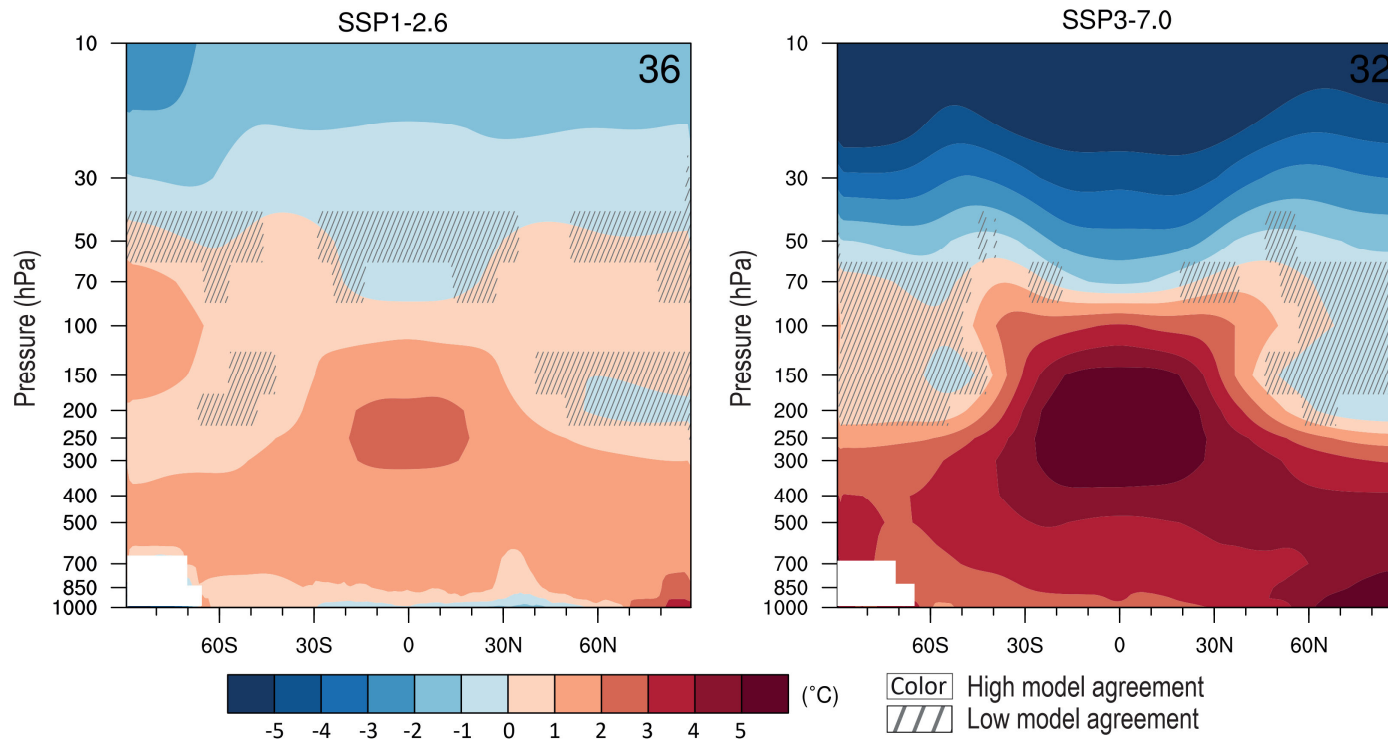


Figure 4.22 | Long-term change of annual and zonal mean atmospheric temperature. Displayed are multi-model mean change in annual and zonal mean atmospheric temperature (°C) in 2081–2100 relative to 1995–2014 for **(left)** SSP1-2.6 and **(right)** SSP3-7.0. The number of models used is indicated in the top right of the maps. Diagonal lines indicate regions where less than 80% of the models agree on the sign of the change and no overlay where 80% or more of the models agree on the sign of the change. Further details on data sources and processing are available in the chapter data table (Table 4.SM.1).

Long-term change of seasonal mean precipitation

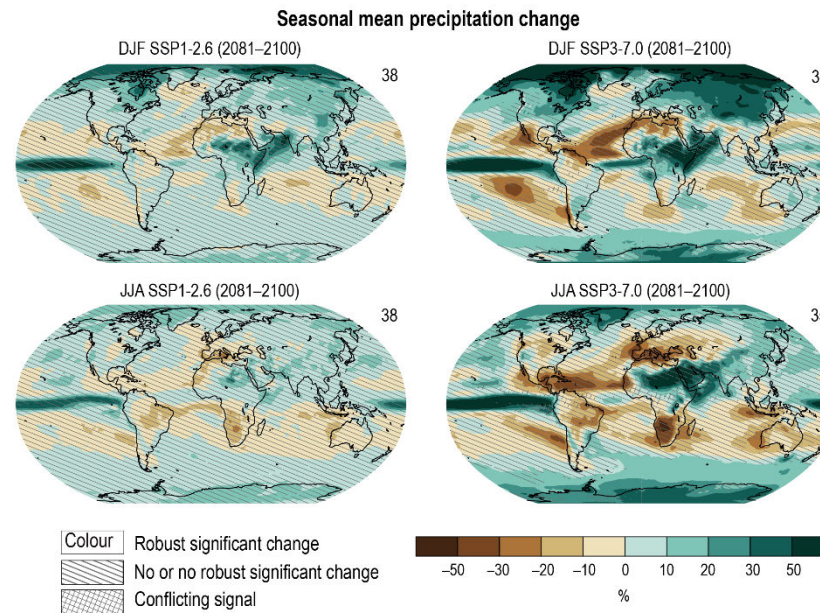


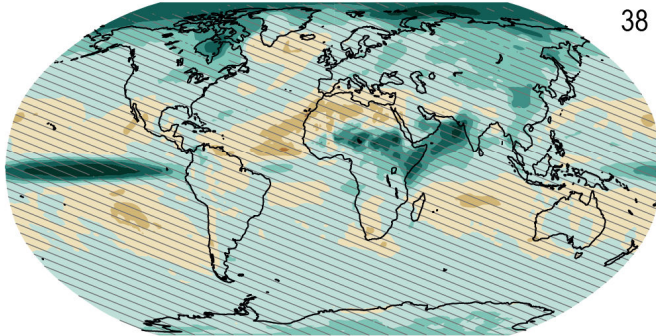
Figure 4.24 | Long-term change of seasonal mean precipitation. Displayed are projected spatial patterns of multi-model mean change (%) in **(top)** December–January–February (DJF) and **(bottom)** June–July–August (JJA) mean precipitation in 2081–2100 relative to 1995–2014, for (left) SSP1-2.6 and (right) SSP3-7.0. The number of models used is indicated in the top right of the maps. No map overlay indicates regions where the change is robust and *likely* emerges from internal variability, that is, where at least 66% of the models show a change greater than the internal-variability threshold (Section 4.2.6) and at least 80% of the models agree on the sign of change. Diagonal lines indicate regions with no change or no robust significant change, where fewer than 66% of the models show change greater than the internal-variability threshold. Crossed lines indicate areas of conflicting signals where at least 66% of the models show change greater than the internal-variability threshold but fewer than 80% of all models agree on the sign of change. Further details on data sources and processing are available in the chapter data table (Table 4.SM.1).



Seasonal mean precipitation change

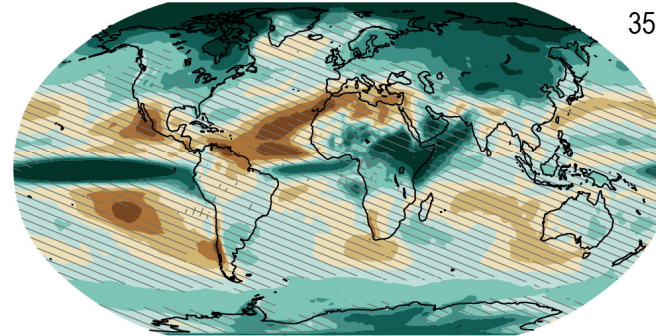
DJF SSP1-2.6 (2081–2100)

38



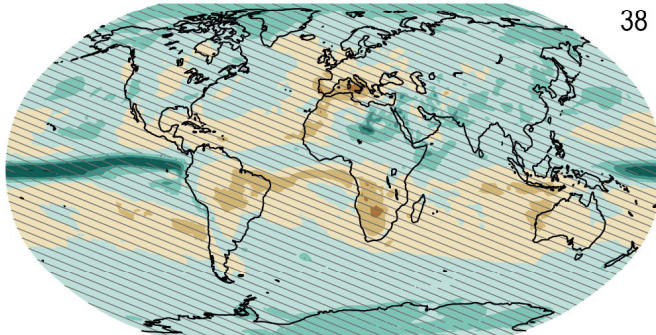
DJF SSP3-7.0 (2081–2100)

35



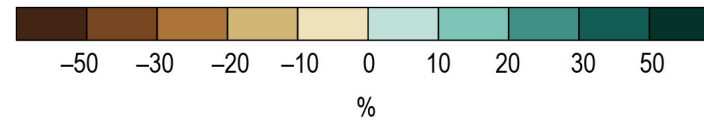
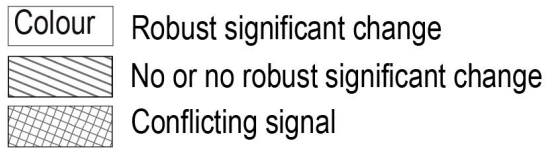
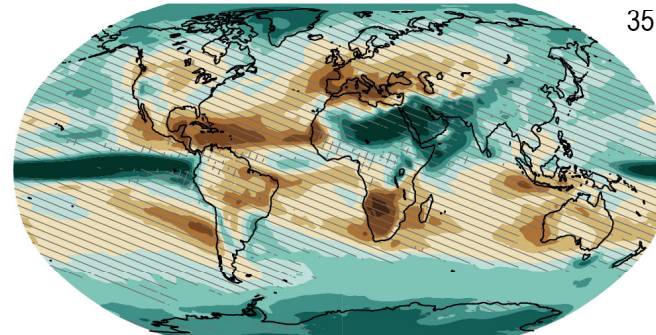
JJA SSP1-2.6 (2081–2100)

38



JJA SSP3-7.0 (2081–2100)

35



Changes in extratropical storm track density

(a) NH DJF 2080-2100 (13)

(b) SH JJA 2080-2100 (13)

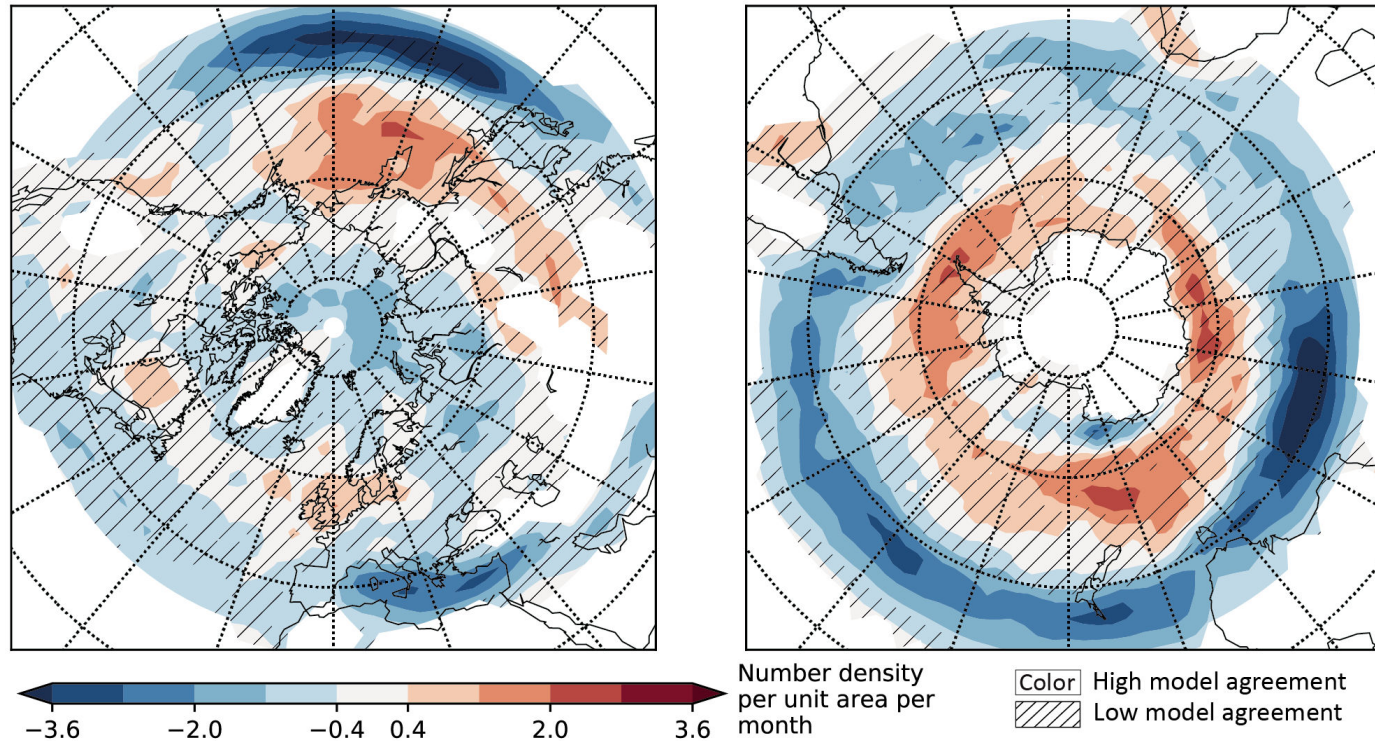
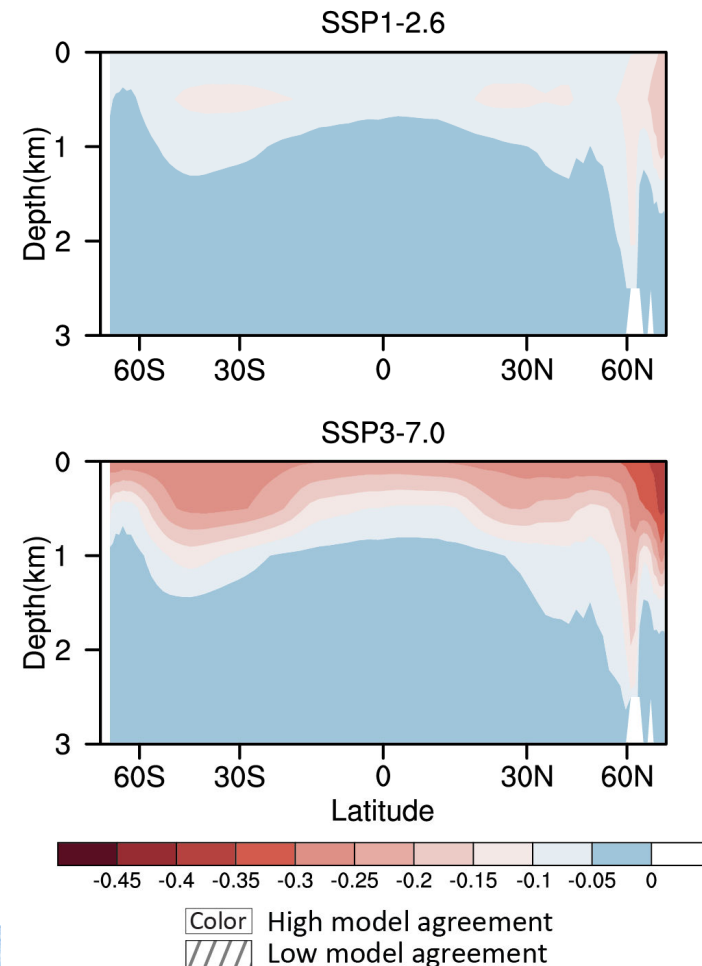


Figure 4.27 | Changes in extratropical storm track density. Displayed are projected spatial pattern of multi-model mean change of extratropical storm track density in winter (Northern Hemisphere December–January–February, NH DJF, and Southern Hemisphere June–July–August, SH JJA) in 2080–2100 for SSP5-8.5 relative to 1979–2014 based on 13 CMIP6 models. Diagonal lines indicate regions where fewer than 80% of the models agree on the sign of the change and no overlay where at least 80% of the models agree on the sign of change. Units are number density per 5° spherical cap per month. Further details on data sources and processing are available in the chapter data table (Table 4.SM.1).

Long-term change of annual and zonal ocean pH

Figure 4.29 | Long-term change of annual and zonal ocean pH. Displayed are multi-model mean change in annual and zonal ocean pH in 2081–2100 relative to the mean of 1995–2014 for SSP1-2.6 and SSP3-7.0, respectively. Eleven CMIP6 model results are used. Diagonal lines indicate regions where fewer than 80% of the models agree on the sign of the change and no overlay where at least 80% of the models agree on the sign of change. Further details on data sources and processing are available in the chapter data table (Table 4.SM.1).



Simulated climate changes up to 2300 under the extended SSP scenarios

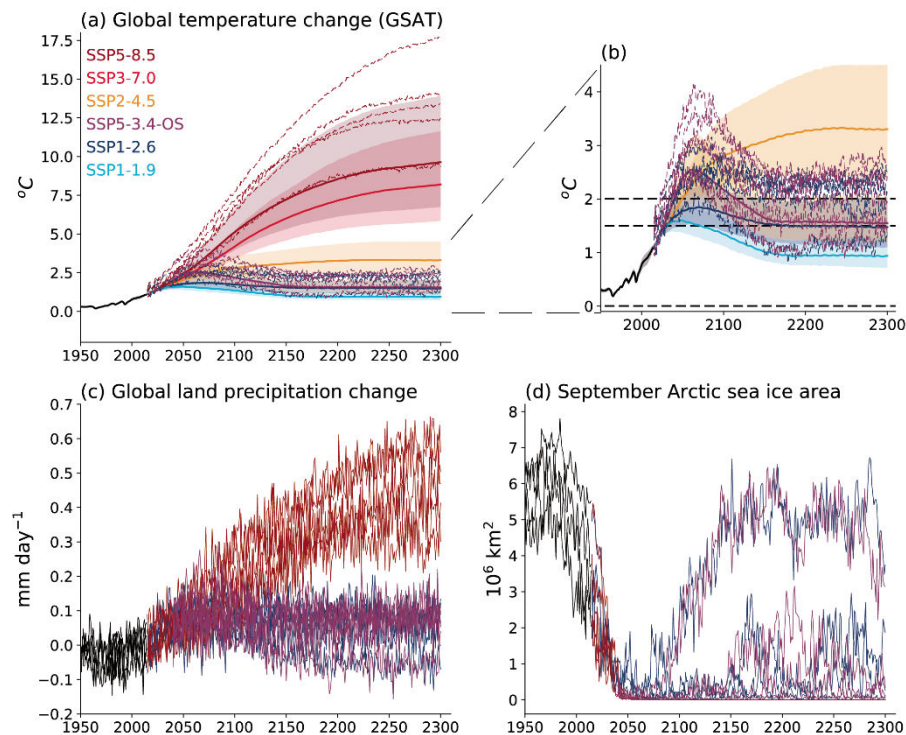
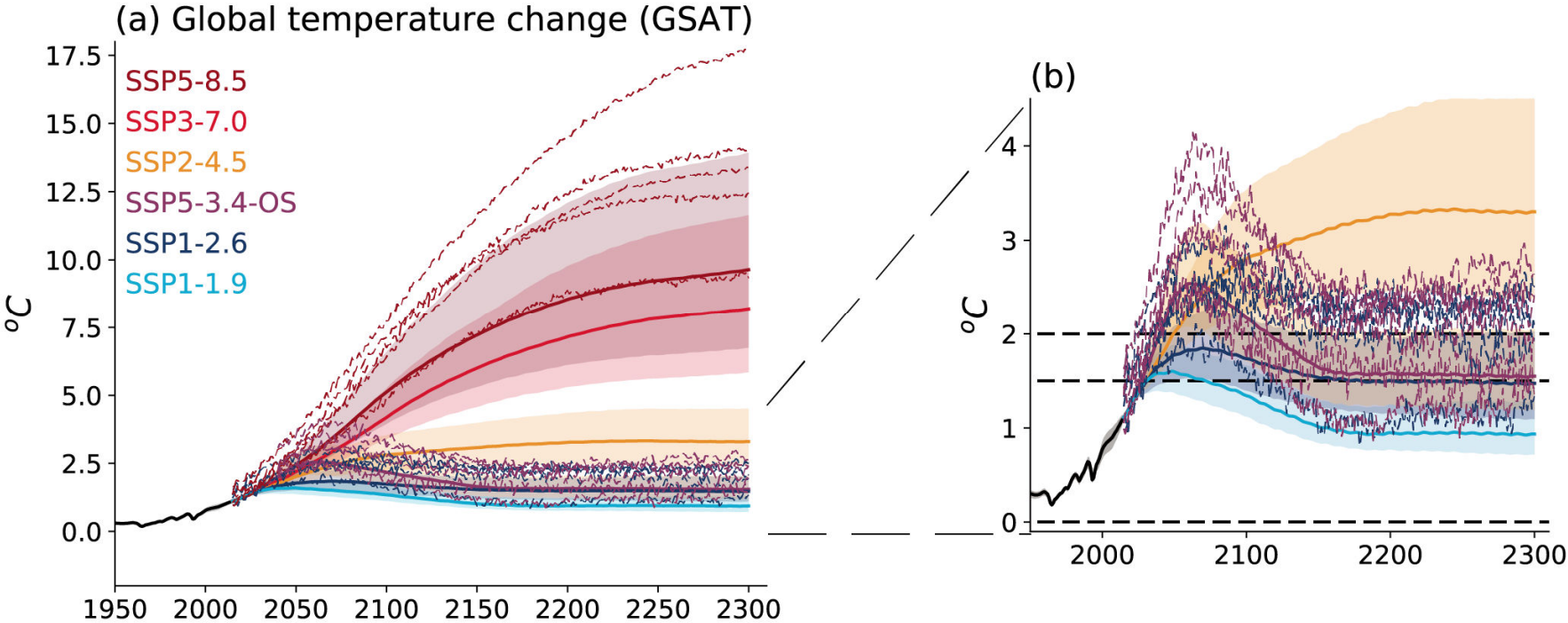
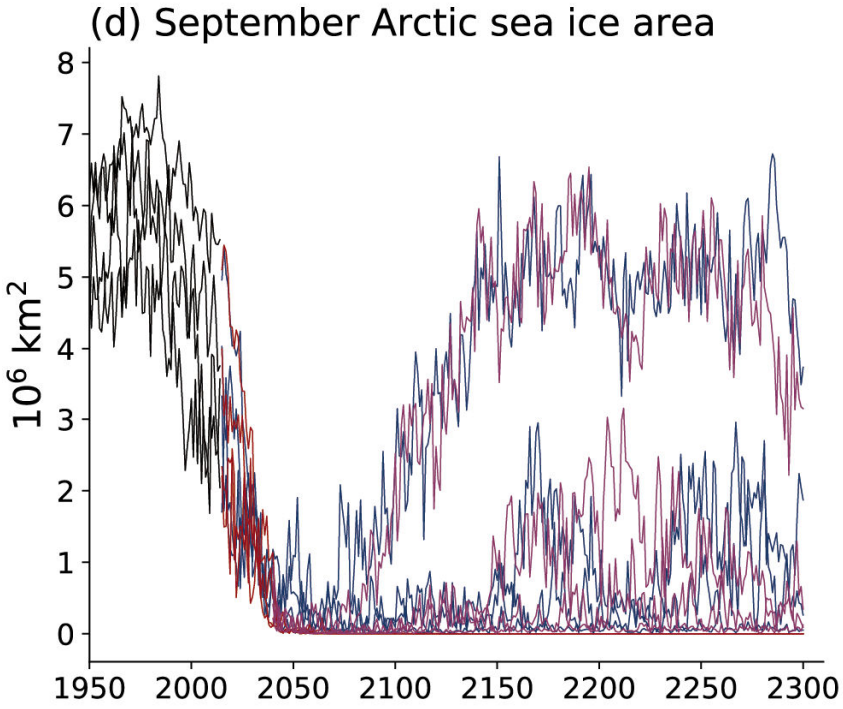
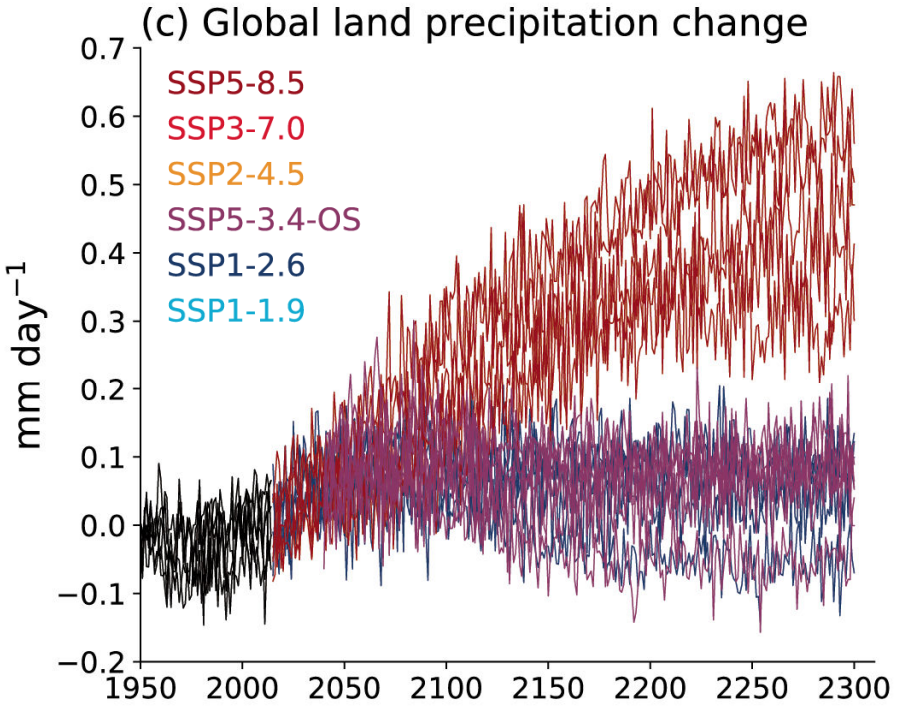


Figure 4.40 | Simulated climate changes up to 2300 under the extended SSP scenarios. Displayed are (a) projected global surface air temperature (GSAT) change, relative to 1850–1900, from CMIP6 models (individual lines) and MAGICC7 (shaded plumes); (b) as (a) but zoomed in to show low-emissions scenarios; (c) global land precipitation change; and (d) September Arctic sea ice area. Further details on data sources and processing are available in the chapter data table (Table 4.SM.1).

Simulated climate changes up to 2300 under the extended SSP scenarios



Simulated climate changes up to 2300 under the extended SSP scenarios



Chapter 5: Global Carbon and other Biogeochemical Cycles and Feedbacks



Knowledge for Tomorrow